Cancer Management and Research

Elevate Series

Open Access Full Text Article

ORIGINAL RESEARCH

Neuroimmunological Mechanisms of Xiao-Yao-San Against Chronic Stress-Induced Colorectal Cancer: A Bioinformatics and Single-Cell Sequencing Study

Ying Li[1,2,*], Shengya Yang[1,2,*], Haoran Li[2], Huachao Li[2], Yunchuan Sun[3], Xinying He[3], Yingru Zhang[1,2,4], Yan Wang[1,2,4]

[1]The Second Clinical Medical College of Guizhou University of Traditional Chinese Medicine, Guiyang, Guizhou Province, 550003, People's Republic of China; [2]Department of Medical Oncology, Shuguang Hospital, Shanghai University of Traditional Chinese Medicine, Shuguang, Shanghai, 201203, People's Republic of China; [3]Oncology Department of Cangzhou Hospital of Integrated TCM-WM, Cangzhou, Hebei Province, 061000, People's Republic of China; [4]School of Integrative Medicine, Shanghai University of Traditional Chinese Medicine, Shanghai, 201203, People's Republic of China

*These authors contributed equally to this work

Correspondence: Yan Wang, The Second Clinical Medical College of Guizhou University of Traditional Chinese Medicine, Guiyang, Guizhou Province, 550003, People's Republic of China, Email yanwang@shutcm.cn; Yingru Zhang, School of Integrative Medicine, Shanghai University of Traditional Chinese Medicine, Shanghai, 201203, People's Republic of China, Email zhangyingru2022@163.com

Objective: This study aimed to integrate bioinformatics, network pharmacology, and single-cell sequencing to explore the potential neuro-immune mechanisms by which the traditional Chinese medicine formula Xiao-Yao-San (XYS) ameliorates chronic stress-induced colorectal cancer (CRC) progression.

Methods: Transcriptomic and survival data of CRC patients were obtained from public databases (TCGA, GEO). Combined with literature review, 130 neurotransmitter-related receptor genes (NRGs) were screened, and their expression and prognostic value in CRC were analyzed. Based on 51 XYS components previously identified by UHPLC/Q-TOF-MS, network pharmacology was employed to predict their potential targets (1,228 in total). These targets were intersected with differentially expressed NRGs. Molecular docking was further performed to evaluate the binding affinity between XYS components and receptors. A mouse model of chronic unpredictable mild stress (CUMS) combined with orthotopic CRC transplantation was established. Neurotransmitter levels were measured by mass spectrometry, and 10x Genomics single-cell transcriptomic sequencing was applied to analyze changes in the tumor immune microenvironment.

Results: Bioinformatics analysis revealed that 100 NRGs were significantly dysregulated in CRC tissues. After intersecting with XYS targets, 14 potential NRGs were identified, among which seven (ADRA2C, DRD1, GABRA2, HTR1B, HTR1D, HTR2A, HTR2B) showed significant correlation with patient prognosis. Molecular docking demonstrated favorable binding activity between XYS components (such as 8-Debenzoylpaeoniflorin and Sucrose) and the hub NRGs. In vivo experiments confirmed that XYS reversed CUMS-induced abnormalities in tumor and plasma levels of norepinephrine, dopamine, and serotonin. Single-cell sequencing further indicated that XYS reduced the CUMS-induced increase in myeloid-derived suppressor cell (MDSC) proportion and modulated the expression of key NRGs, including HTR2A in macrophages and HTR1B in T cells. KEGG enrichment analysis suggested that neuroactive ligand-receptor interaction and immune-related pathways were significantly regulated upon XYS intervention.

Conclusion: XYS modulates neurotransmitter homeostasis and the tumor immune microenvironment in CRC under chronic stress through a multi-component and multi-target manner, which is closely associated with the regulation of key NRGs such as HTR1B and DRD1. This study provides neuro-immunological evidence for the clinical application of XYS in CRC patients with emotional disorders.

Keywords: Xiao-Yao-San, colorectal cancer, neuroimmunological mechanisms, single-cell sequencing, network pharmacology

Introduction

Colorectal cancer (CRC) is a globally prevalent malignant gastrointestinal tumor, and its incidence and progression are influenced by a variety of factors, including emotions, diet, inflammation, medication use, and genetics.[1,2] Chronic stress,

https://doi.org/10.2147/CMAR.S567746
Received: 19 October 2025
Accepted: 20 February 2026
Published: 3 March 2026

arising from the accumulation of negative emotions such as long-term anxiety, depression, and persistent pressure, has been found to increase the risk of depressive symptoms in cancer patients by five times compared to the general population.[3] Under the negative impact of chronic stress, CRC patient survival prognosis is often unfavorable. Numerous studies have demonstrated that chronic stress disrupts the integrity of the intestinal barrier,[4] causes an imbalance in gut microbiota,[5] interferes with the normal functioning of the immune system,[6] and remodels the tumor microenvironment (TME) toward immunosuppression.[7,8] These mechanisms collectively promote the occurrence and development of CRC. Therefore, the negative impact of chronic stress on CRC progression warrants further investigation. Our previous studies have also shown that antidepressants can significantly modulate gut microbiota and TME composition, thereby inhibiting CRC development.[9]

In recent years, the neuro-immune axis has increasingly become a focal point of attention among numerous researchers. The nervous system plays a critical role in regulating immune cells by controlling their activation, proliferation, and distribution, thereby influencing the normal function of the immune system.[10] The gut is one of the target organs in both the nervous and immune systems and holds a crucial position in explaining the occurrence and progression of CRC (Colorectal Cancer) under chronic stress. Chronic stress induces multiple mechanisms connecting the nervous system with the CRC immune microenvironment, including the brain-gut axis formed by the hypothalamic-pituitary-adrenal axis (HPA axis) in the central nervous system and the autonomic nervous system (eg, the sympathetic-adrenal medullary axis, SAM axis), as well as the enteric nervous system (ENS) unique to the intestinal wall.[11] These systems regulate immune cells within the TME by producing and releasing neurotransmitters, neuropeptides, and neurotrophic factors.[6] For instance, 5-hydroxytryptamine (5-HT), a neurotransmitter produced under chronic stress, influences various immune cells in the TME, such as T cells, B cells, NK cells, macrophages, and neutrophils,[12] thereby creating an immunosuppressive microenvironment that accelerates the rapid development of CRC.[13] Our previous research has demonstrated that chronic stress can induce the formation of an immunosuppressive microenvironment, promoting the development of CRC.[14]

Xiao-Yao-San (XYS), originating from the *Taiping Huimin Heji Jufang* (*Formulary of the Bureau of People's Welfare Pharmacy*) of the Song Dynasty, is composed of *Angelica sinensis (Danggui), Paeonia lactiflora (Baishao), Bupleurum chinense (Chaihu), Poria cocos (Fuling), Atractylodes macrocephala (Baizhu), Glycyrrhiza uralensis (Gancao), Mentha haplocalyx (Bohe), and Zingiber officinale (Shengjiang). It is a representative formula in traditional Chinese medicine for the treatment of psychological disorders. Compared with conventional antidepressant drugs, XYS maintains comparable efficacy while inducing fewer adverse effects*,[15,16] making it more suitable for long-term use in cancer patients with comorbid emotional disturbances, thereby potentially improving patient survival and quality of life.[17] Current research suggests that XYS exerts its antidepressant effects through multiple biological processes, including the modulation of monoamine neurotransmitter transport,[18] regulation of the HPA axis,[19] regulation of neuroplasticity,[20] and synaptic plasticity,[21] reduction of inflammatory responses,[22] neuroprotection,[23] modulation of the gut-brain axis,[24] regulation of gut microbiota,[25,26] and modulation of oxidative stress and autophagy to reduce neuronal apoptosis.[27,28] These effects highlight the unique multi-layered, multi-pathway, and multi-target advantages of traditional Chinese herbal medicine.[29]

Our previous studies have confirmed that XYS exhibits excellent regulatory and ameliorative effects in CRC mice under chronic stress by modulating the abundance of *Bacteroides, Lactobacillus, Desulfovibrio*, and *Rikenellaceae* to restore disrupted gut microbiota, thereby effectively suppressing CRC progression.[30] In this process, we observed that XYS also significantly influenced serum neurotransmitter levels and immune cell functions in the mice. This led us to propose a hypothesis: whether the regulatory effect of XYS in CRC mice with chronic stress is mediated via the neuro-immune axis. However, studies on whether XYS affects the CRC immune microenvironment by regulating neurotransmitter-related receptors remain unsystematic, lacking analysis at the single-cell level regarding immune cell subsets and their expression of neurotransmitter receptors. Conventional "bulk" transcriptome sequencing falls short in revealing the heterogeneous responses of different immune cell subsets within the tumor microenvironment (TME) to neural signals, whereas single-cell RNA sequencing provides a high-resolution approach for such investigations. Therefore, by integrating bioinformatics and network pharmacology, we predicted the targets of the XYS components previously identified via UHPLC/Q-TOF-MS analysis. These predicted targets were intersected with neurotransmitter-related receptor genes collected through extensive literature review, followed by molecular docking validation. Combining bio-sample data

from public databases with serological assays and single-cell sequencing results from laboratory animal models, we conducted a preliminary exploration of the therapeutic efficacy of XYS in CRC mice with chronic stress from the perspective of the neuro-immune axis. This study provides a novel perspective on the multi-target mechanisms of traditional Chinese medicine formulations in cancer therapy.

Material and Methods

Main Experimental Reagents and Instrumentation

XYS: *Angelica sinensis* (Danggui), *Paeonia lactiflora* (Baishao), *Bupleurum chinense* (Chaihu), *Poria cocos* (Fuling), *Atractylodes macrocephala* (Baizhu), *Glycyrrhiza uralensis* (Gancao), *Mentha haplocalyx* (Bohe), and *Zingiber officinale* (Shengjiang). (supplied by the Affiliated Hospital of the Shanghai University of Traditional Chinese Medicine, Shanghai, China), Fluoxetine Hydrochloride Capsules (FXT, Patheon France, 22301AC);Wide-field Experimental video analysis system (Shanghai Xinsoft, XR-XZ301), ultra-high performance liquid chromatography (Waters Acquity, Waters, USA), triple quadruple mass spectrometer (AB Sciex, API5500, USA), fluorescence microscope (Leica, DM2500, Germany); PubChem database (https://pubchem.ncbi.nlm.nih.gov/), PharmMapper database (https://www.lilab-ecust.cn/pharmmapper/), Cytoscape 3.10.3 software, PyMOL software (Version 2.4), Chem3D software, AutoDockTools software (Version 1.5.6), AutoDock Vina software, R language (x64 4.2.3); Perl language (Strawberry 5.32).

Bioinformatics Analysis

We collected sample data and clinical information from healthy individuals and CRC patients from the TCGA and GEO databases, selecting the GSE71187 dataset that includes healthy controls, CRC samples, and survival information for our study. This selection yielded data from 56 healthy individuals and 618 CRC patients, along with 623 pieces of prognostic survival information. Initially, we verified whether the neurotransmitter-related receptor genes (NRGs) obtained through literature retrieval exhibit differential expression between healthy and tumor tissues. After merging tumor samples from both databases, we performed univariate COX analysis on the significantly expressed NRGs to identify genes associated with prognosis. Subsequently, we validated their prognostic value using Kaplan-Meier survival analysis.

Preparation of XYS Extract

XYS herbs were weighed and then dissolved in an 8-fold volume of pure water. They were subsequently heated and simmered for 1 hour twice. The mixture was then heated under reflux for 1 hour using a rotary evaporator (55 rpm, 90°C, 0.8 MPa) to extract the aqueous solvent. The filtrate was filtered through 8 layers of cheesecloth. The extract was then divided into low- and high-dose groups based on the oral dosage of humans. According to a body surface area conversion factor, the administered dose for mice was 9.1 times that of humans. Based on the experimental design, the high-dose group received twice the daily human oral dose, while the low-dose group received half of the high-dose dose, resulting in a daily administered volume of 30.77 mL for the high-dose group and 15.38 mL for the low-dose group.

Molecular Docking

Based on the UHPLC/Q-TOF/MS analysis, the primary components of XYS were identified, and their chemical structures were retrieved from the PubChem database and downloaded. Target gene matching was conducted using the PharmMapper database to determine the interaction between the compounds and neurotransmitter-related receptors. The molecular structures of the small molecule components were optimized using Chem3D software. A comprehensive literature search was performed to identify neurotransmitter-related receptor genes, and their PDB format files were downloaded from the PDB database. A Venn diagram was constructed to visualize the intersection of these genes, thereby establishing potential interaction relationships between the small molecule compounds and neurotransmitter-related receptors. Molecular docking simulations and binding energy calculations were performed using AutoDock Tools software, with the results visualized using PyMol software to provide a detailed molecular interaction analysis.

Cell Line Cultivation

The human CRC cell line CT26 was purchased from the Chinese Academy of Sciences and is stored at the Institute of Oncology, Shuguang Hospital Affiliated with Shanghai University of Traditional Chinese Medicine. The cells were verified through STR profiling and were cultured in an environment at 37°C with 5% CO_2.

Animal Model Preparation

Referring to established and validated protocols for chronic stress modeling in mice, a chronic unpredictable mild stress (CUMS) paradigm was employed.[31] Twenty 4-week-old male BALB/c mice were randomly divided into four groups (control group, model group, XYS group, and fluoxetine group), with five mice per group. This sample size was determined based on previous studies using similar stress-induced colorectal cancer models, which have consistently demonstrated sufficient statistical power (α=0.05, β=0.8) for detecting differences in tumor volume and immune markers. All mice were housed at the Experimental Animal Center of Shanghai University of Traditional Chinese Medicine. The animal experiment protocol complied with the *National Standard for the Use of Experimental Animals (China)* and was approved by the Ethics Committee of Shanghai University of Traditional Chinese Medicine (approval number: PZSHUTCM220913004). After two weeks of continuous CUMS induction, an orthotopic CRC tumor model was established by injecting 40 μL of CRC cell suspension (5×10^7 cells/mL) into the intestinal wall via rectal needle puncture. CUMS induction was then continued for another three weeks, during which mice in the XYS and fluoxetine groups received daily intragastric administration of the corresponding treatment.

Behavioral Testing

To evaluate the behavioral responses of the experimental mice, four behavioral tests were conducted: Open Field Test (OFT),Tail-Fixing Test (TST), and Forced Swimming Test (FST).[32,33] The specific implementation plans were as follows:

Open Field Test (OFT)

Test mice were individually housed in a quiet environment for 30 minutes to acclimate to the testing conditions. After acclimatization, mice were placed in the center of an open field apparatus for 5 minutes. The behavior of the mice was recorded using video cameras, focusing on parameters such as the number of entries into the central area, total movement distance, and duration of static periods. The behavioral scores were calculated based on the aforementioned parameters. A higher number of central entries, longer movement distances, and shorter static periods indicate reduced anxiety and increased spontaneous activity. Conversely, a lower number of central entries, shorter movement distances, and longer static periods suggest heightened anxiety and decreased spontaneous activity.

Tail Suspension Test (TST)

The last third of the mouse's tail was taped and suspended in an apparatus 30 cm above the ground, ensuring the mouse could not touch the floor. Two experimenters observed and recorded the mouse's stationary and struggling times for 5 minutes.

Forced Swim Test (FST)

Mice were placed in a water tank with a water temperature of 23±1°C, and two experimenters observed and recorded the mouse's swimming and stationary times for 6 minutes.

Neurotransmitter Analysis in Mouse Tumor and Plasma Samples Using Mass Spectrometry

When anesthetizing and collecting blood using intraperitoneal injection of 1% pentobarbital sodium, and then euthanizing animals by intraperitoneal injection of pentobarbital sodium at three times the anesthetic dose for animal sampling. For quantitative analysis of major neurotransmitters, 100 μL of mouse tumor and plasma samples were mixed with 300 μL of methanol. The mixture was vortexed for 3 min and centrifuged at 12,000 rpm for 10 min. The supernatant

(100 μL) was then transferred and supplemented with 20 μL of internal standard solution (carbamazepine at 211 ng/mL) prior to injection. A volume of 0.5 μL was loaded for analysis.

Preparation of Single-Cell Suspension

Fresh intestinal tumor tissues were collected from experimental mice and washed twice with pre-cooled RPMI-1640 medium under sterile conditions. The tissues were then cut into small fragments of approximately 0.5 mm^3. Subsequent enzymatic digestion was performed with collagenase at 37°C for 60 min in a shaking incubator, with gentle mixing every 5–10 min. The resulting cell suspension was filtered through a 40 μm cell strainer to remove debris. The filtrate was centrifuged, and the cell pellet was resuspended in an equal volume of red blood cell lysis buffer for 10 min. After red blood cell separation and centrifugation, the cells were washed once with 1×PBS. Finally, the cell pellet was resuspended in an appropriate volume of culture medium, and cell concentration and viability were determined using an automated cell counter.

Single-Cell RNA Sequencing Analysis of Tumor Tissue

Fresh tumor tissue was prepared as a single-cell suspension at a concentration of 1×10^6 cells/mL and encapsulated in water-in-oil emulsion droplets. Fresh tumor/intestinal tissue was collected from mice using surgical scissors. Single-cell capture was performed using the 10× Genomics Chromium platform. cDNA synthesis and PCR amplification were conducted according to the instructions provided in the 10×Genomics Chromium Next GEM Single Cell 3' Reagent Kits v3.1 (catalog number: 1000268). The sequencing library was constructed using the NEBNext Ultra II DNA Library Prep Kit, and high-throughput sequencing was performed on the Illumina NovaSeq 6000 platform with a target read length of 150 bp paired-end.

The raw sequencing data generated in FASTQ format were processed using Cell Ranger software (v6.0) and the Seurat package. The processing included identifying the barcode tags that distinguish cells and the UMI tags corresponding to different mRNA molecules within each cell. Quantification of high-throughput single-cell transcriptomic data was performed, and low-quality reads and barcodes were removed to obtain quality control information such as high-quality cell count, gene median, and sequencing saturation. The specific quality control criteria were as follows: cells with fewer than 200 genes were removed, and cells with UMI counts greater than 1000, log10GenesPerUMI less than 0.7, mitochondrial gene expression less than 5%, and red blood cell gene expression less than 5% were retained as high-quality cells. DoubletFinder software was used to remove doublets.

For data analysis, the MNN (mutual nearest neighbors) algorithm was first applied to remove batch effects. Based on the MNN-reduced data, the UMAP (Uniform Manifold Approximation and Projection) algorithm was used for single-cell cluster visualization, and the SNN clustering algorithm was applied to identify optimal cell clusters. The FindVariableGenes function in the Seurat package was used to identify marker genes. The SingleR package was employed to annotate and classify cell clusters by calculating the Spearman correlation between the expression profiles of the cells to be identified and reference datasets from public databases. Additionally, the FindMarker function was used to perform differential expression analysis, with FDR < 0.05 and an absolute fold change of >1.5 as the thresholds to identify differentially expressed immune cells with characteristic changes between groups. The detailed experimental workflow is shown in Figure 1.

Results

Literature Search and Selection of Receptor Genes (NRGs) Related to Major Neurotransmitters

Mechanisms of Neuro-Immune Interaction are Mediated Through Alterations in Neurotransmitters, Neuropeptides, and Neurotrophic Factors. As the most common neural regulators, neurotransmitters have been extensively implicated in the modulation of the immune system in colorectal cancer. Therefore, through a comprehensive literature review, we selected classical neurotransmitters, including glutamate (Glu),[34] γ-Aminobutyric Acid (GABA),[35] Glycine,[36] Histamine,[37] Epinephrine (EPI), Norepinephrine (NE), Dopamine (DA), 5-HT, and Acetylcholine (ACh) as shown in Table 1. These neurotransmitters were associated with a total of 130 relevant receptor genes, as shown in Table Principal Component Results of XYS Herbal Formula.

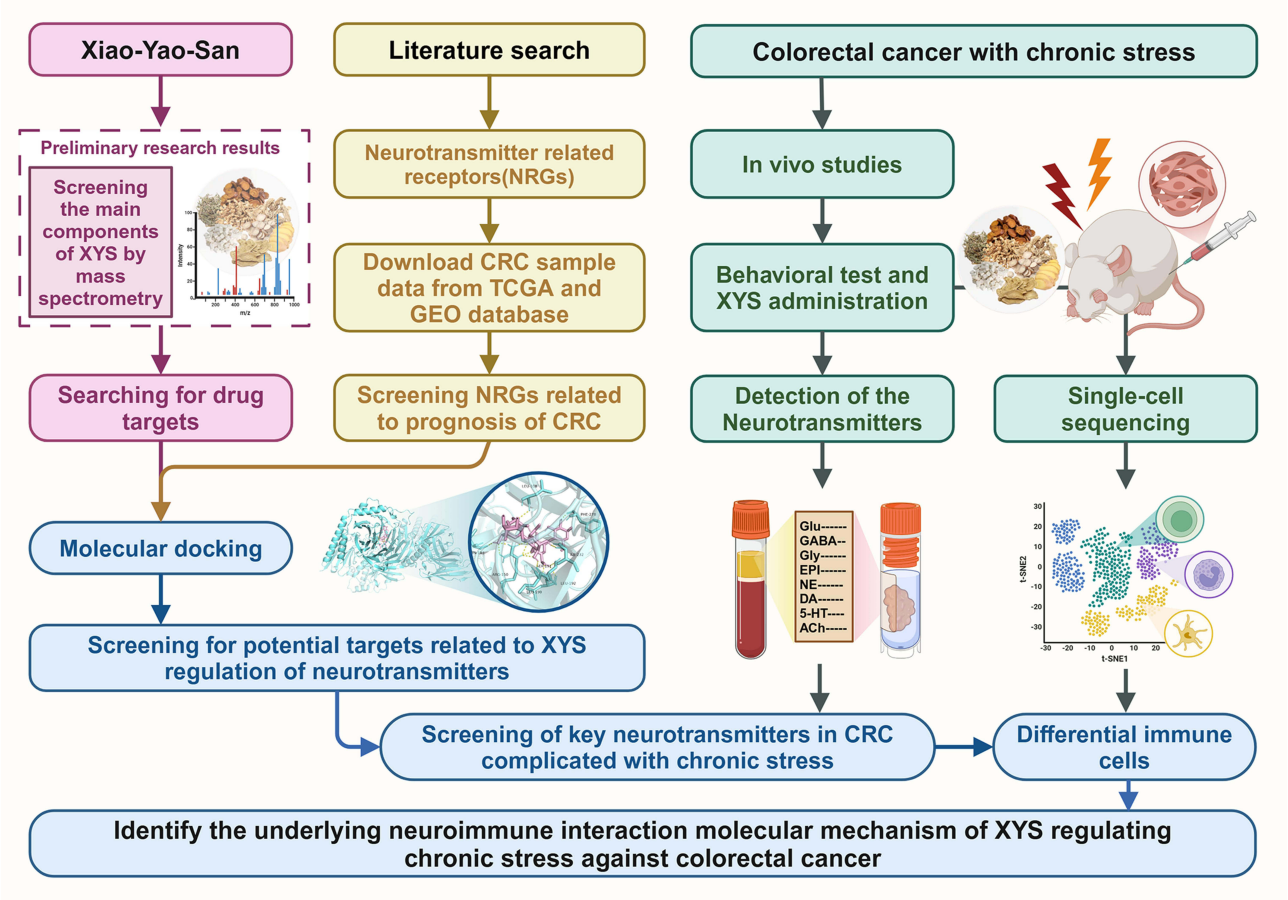

Figure 1 The flow chart.

In our previous studies, the chemical constituents of the XYS traditional Chinese medicine compound were analyzed using ultra-high performance liquid chromatography coupled with quadrupole time-of-flight mass spectrometry (UHPLC/Q-TOF/MS) method. Detailed information regarding the analytical methodology can be found in (PMID: 33113425).[30]

Table 1 The Gene List of Major Neurotransmitter-Related Receptors

Major Neurotransmitters	Related Receptor Genes
Glutamate	GRIA1, GRIA2, GRIA3, GRIA4, GRID1, GRID2, GRID2IP, GRIK1, GRIK2, GRIK3, GRIK4, GRIK5, GRIN1, GRIN2A, GRIN2B, GRIN2C, GRIN2D, GRIN3A, GRIN3B, GRINA, GRIP1, GRIP2, GRIPAP1, GRM1, GRM2, GRM3, GRM4, GRM5, GRM6, GRM7, GRM8
Glycine	GLRA1, GLRA2, GLRA3, GLRA4
Histamine	HRH1, HRH2, HRH3, HRH4
Epinephrine and norepinephrine	ADRA1A, ADRA1B, ADRA1D, ADRA2A, ADRA2B, ADRA2C, ADRB1, ADRB2, ADRB3
Dopamine	Drd1, Drd2, DRD3, DRD4, DRD5
5-HT	HTR1A, HTR1B, HTR1D, HTR1E, HTR1F, HTR2A, HTR2B, HTR2C, HTR3A, HTR3B, HTR3C, HTR3D, HTR3E, HTR4, HTR5A, HTR6, HTR7, HTR7P1, SLC6A4, SLC18A1
GABA	GABBR1, GABBR2, GABRA1, GABRA2, GABRA3, GABRA4, GABRA5, GABRA6, GABRB1, GABRB2, GABRB3, GABRD, GABRE, GABRG1, GABRG2, GABRG3, GABRP, GABRQ, GABRR1, GABRR2, GABRR3
Acetylcholine	CHRM1, CHRM2, CHRM3, CHRM4, CHRM5, CHRNA1, CHRNA2, CHRNA3, CHRNA4, CHRNA5, CHRNA6, CHRNA7, CHRNA8, CHRNA9, CHRNA10, CHRNB1, CHRNB2, CHRNB3, CHRNB4, CHRND, CHRNE, CHRNG, AChR, ChAT, AGLRP4, DOK7, MUSK, RAPSN, PREPL, MYO9A, SCN4A, PLEC1, SLC25A1, COLQ, SLC18A3, GFPT1

Based on the multi-level mass spectrometry data, combined with the Natural Products High-Resolution Mass Spectrometry Database and relevant literature, a total of 51 compounds were identified in XYS. Among these, the most abundant components were guanosine (Guanosine), gallic acid (Gallic acid), paeoniflorin (Paeoniflorin), glycyrrhizic acid (Glycyrrhizic acid), and buddleoside (Buddleoside), as listed in Supplementary Table 1.

To predict the potential molecular targets of these compounds, the PharmMapper database was utilized. Out of the 51 compounds identified by UHPLC/Q-TOF/MS, 2 compounds were not recorded in the PubChem database, and 3 compounds could not have their potential targets predicted by PharmMapper, thus they were excluded from further analysis. Consequently, a total of 1,228 potential drug targets were identified for the 46 major components of the XYS compound. A "Herb-Compound-Drug Target" network diagram was constructed to illustrate the correspondence between the components, their herbal origins, and their predicted molecular targets, as shown in Figure 2.

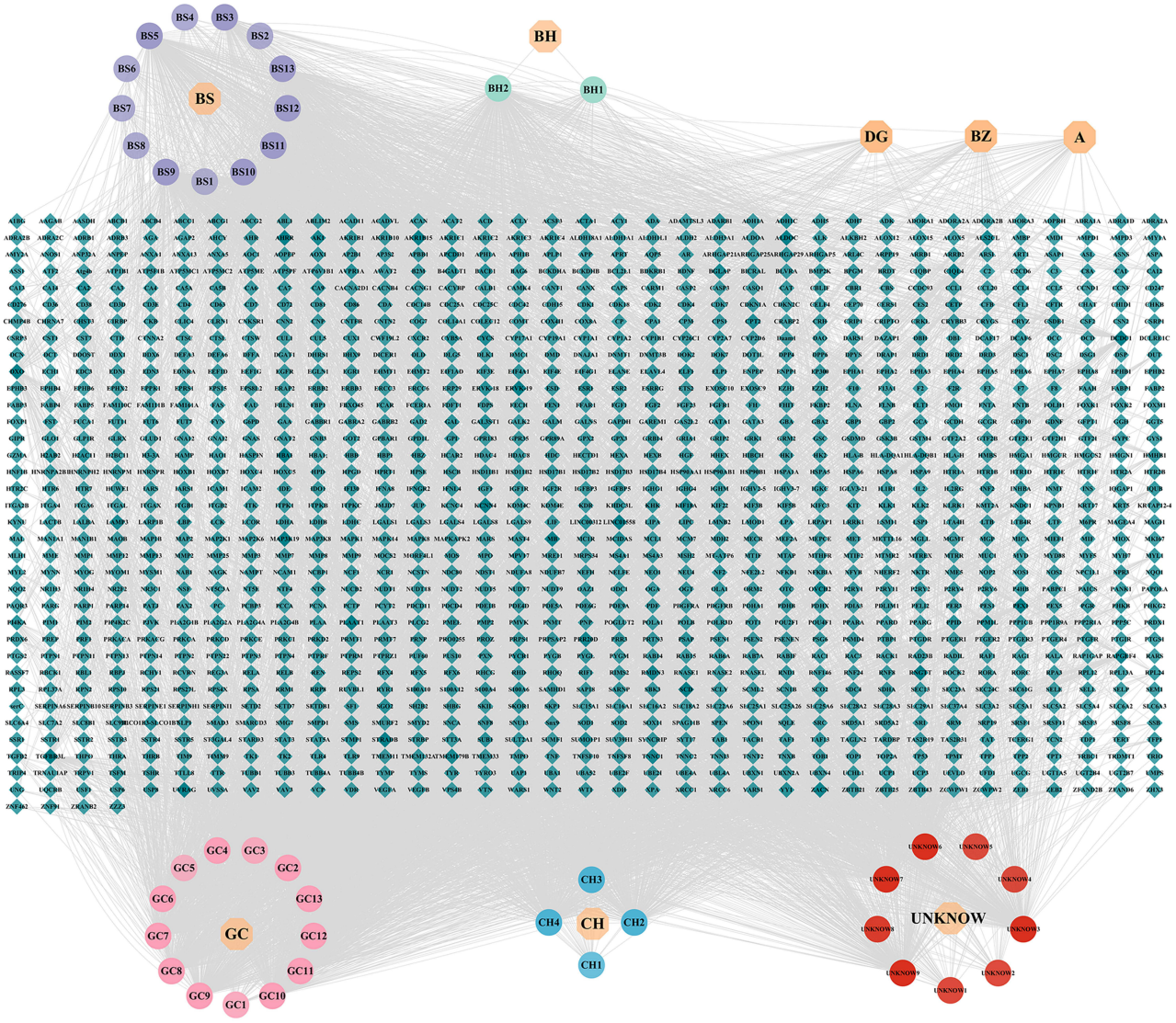

Figure 2 Network diagram of "Traditional Chinese Medicine-Ingredients-Drug targets" of Xiao-Yao-San. In the figure, the octagonal symbols represent the traditional Chinese medicines composing XYS, the circular symbols denote the components identified by UHPLC/Q-TOF/MS, and the diamond-shaped symbols indicate the potential drug targets. The depth of the symbols' shading represents the Count value in the network diagram, with darker colors indicating more complex drug-target interaction relationships.

https://doi.org/10.2147/CMAR.S567746

Molecular Docking

Further intersection analysis was conducted between the XYS compound components and the literature-acquired NRGs. According to the Venn diagram, a total of 31 genes were identified as potential NRGs targeted by XYS. To validate the binding interactions between these genes and the herbal compounds, molecular docking simulations were performed. Due to the absence of the receptor structure for GABRA2 in the Protein Data Bank (PDB), molecular docking simulations were conducted for the remaining 27 receptors corresponding to the other genes, excluding GABRA2, SLC25A1, ADRA1D, and DOK7. The results of these simulations are presented in Table 2, a total of 70 binding combinations were identified between XYS and hub-NRGs, with over half of these combinations exhibiting binding energies of less than −7 kcal/mol. This indicates a widespread and strong binding relationship between XYS and the NRGs. The top 12 binding combinations, ranked by binding energy, were selected for further analysis, and their docking modes are illustrated in Figure 3.

Table 2 Summary Table of Docking Results Between Compound Components in XYS and NRGs

Ingredient Number	Ingredient Name	Gene Name	Related Neurotransmitters	Herbal Medicine of Ingredient Origin	Binding Energy (kcal/mol)
7	Maltopentaose	ADRB3	NE	/	−10.8
33	Buddleoside	GFPT1	ACh	BH	−10.5
42	Licorice saponin E2	HTR1E	5-HT	GC	−10.2
40	Macedonoside A	HTR1E	5-HT	GC	−10.0
14	6'-O-Galloylsucrose	HTR1F	5-HT	BS	−9.9
42	Licorice saponin E2	ADRA2A	NE	GC	−9.6
47	Saikosaponin A	DRD2	DA	CH	−9.6
49	Uralsaponin B	DRD2	DA	GC	−9.4
50	2''-O-acetylsaikosaponin D	DRD2	DA	CH	−9.4
20	Albiflorin	HTR1E	5-HT	BS	−9.4
25	Galloylpaeoniflorin	DRD2	DA	BS	−9.3
38	Licoricesaponin A3	HTR1E	5-HT	GC	−9.1
38	Licoricesaponin A3	DRD2	DA	GC	−9.0
48	Saikosaponin D	DRD2	DA	CH	−8.9
27	Mudanpioside I	ADRA2A	NE	BS	−8.8
48	Saikosaponin D	ADRA2A	NE	CH	−8.7
46	Glycyrrhizic acid	DRD2	DA	GC	−8.7
38	Licoricesaponin A3	ADRA2A	NE	GC	−8.6
5	8-Debenzoylpaeoniflorin	ADRA2B	NE	BS	−8.6
24	Liquiritin apioside	HTR1E	5-HT	GC	−8.4
40	Macedonoside A	DRD2	DA	GC	−8.3
34	Licorice saponin J2	DRD2	DA	GC	−8.2
2	Sucrose	ADRA2B	NE	/	−8.0
36	Benzoylpaeoniflorin	HTR1E	5-HT	BS	−8.0
42	Licorice saponin E2	DRD2	DA	GC	−7.8
5	8-Debenzoylpaeoniflorin	DRD3	DA	BS	−7.8
14	6'-O-Galloylsucrose	DRD2	DA	BS	−7.7
47	Saikosaponin A	ADRA2A	NE	CH	−7.6
21	Paeoniflorin	HTR1E	5-HT	BS	−7.6
24	Liquiritin apioside	DRD2	DA	GC	−7.4
2	Sucrose	DRD3	DA	/	−7.0
5	8-Debenzoylpaeoniflorin	ADRA2C	NE	BS	−6.9
5	8-Debenzoylpaeoniflorin	HTR2B	5-HT	BS	−6.9
5	8-Debenzoylpaeoniflorin	ADRA1A	NE	BS	−6.8

(*Continued*)

Table 2 (Continued).

Ingredient Number	Ingredient Name	Gene Name	Related Neurotransmitters	Herbal Medicine of Ingredient Origin	Binding Energy (kcal/mol)
8	Maltohexaose	GRIP2	Glu	/	−6.8
2	Sucrose	ADRA1A	NE	/	−6.7
5	8-Debenzoylpaeoniflorin	DRD1	DA	BS	−6.6
2	Sucrose	ADRA2C	NE	/	−6.5
15	Tryptophan	ADRB1	NE	/	−6.5
5	8-Debenzoylpaeoniflorin	HTR1B	5-HT	/	−6.5
15	Tryptophan	HTR1D	5-HT	/	−6.5
2	Sucrose	HTR6	5-HT	/	−6.3
5	8-Debenzoylpaeoniflorin	DRD2	DA	BS	−6.2
5	8-Debenzoylpaeoniflorin	HTR2A	5-HT	BS	−6.2
15	Tryptophan	ADRA2A	NE	/	−6.0
15	Tryptophan	HTR1A	5-HT	/	−5.9
15	Tryptophan	HTR7	5-HT	/	−5.9
2	Sucrose	HTR2C	5-HT	/	−5.7
5	8-Debenzoylpaeoniflorin	ADRA2A	NE	BS	−5.6
2	Sucrose	DRD1	DA	/	−5.6
2	Sucrose	DRD2	DA	/	−5.6
1	Quinic acid	GABRB2	GABA	/	−5.6
2	Sucrose	HTR2B	5-HT	/	−5.5
5	8-Debenzoylpaeoniflorin	HTR6	5-HT	BS	−5.5
15	Tryptophan	HTR1E	5-HT	/	−5.3
15	Tryptophan	HTR6	5-HT	/	−5.3
1	Quinic acid	CHRNA7	ACh	/	−5.0
15	Tryptophan	GRIA1	Glu	/	−5.0
15	Tryptophan	HTR2B	5-HT	/	−5.0
15	Tryptophan	GABBR1	GABA	/	−4.9
15	Tryptophan	HTR2A	5-HT	/	−4.9
2	Sucrose	ADRA2A	NE	/	−4.8
15	Tryptophan	SLC6A4	5-HT	/	−4.8
41	Pinellic acid	GRM2	Glu	BZ	−4.6
3	Citric acid	CHRNA7	ACh	BS	−4.5
15	Tryptophan	HTR1B	5-HT	/	−4.3
2	Sucrose	HTR1B	5-HT	/	−4.1
41	Pinellic acid	SLC6A4	5-HT	BZ	−4.1
1	Quinic acid	GABBR1	GABA	/	−3.9
2	Sucrose	HTR2A	5-HT	/	−1.4

Screening of Hub-NRGs

Through bioinformatic analysis of CRC sample data from the TCGA and GEO databases, we observed that TCGA data revealed significant differential expression of 100 out of 130 NRGs between healthy controls and CRC patients, suggesting that alterations in neurotransmitter levels and receptor activation are common phenomena in CRC patients, as shown in Figure 4A and SFigure 1A–D. Similarly, differential expression analysis of the GEO dataset identified 58 overlapping NRGs, as illustrated in Figure 4B and SFigure 1E. By performing a second intersection analysis between the differentially expressed NRGs from both databases and the NRGs targeted by XYS, we ultimately identified 14 NRGs that XYS may potentially regulate in CRC, as shown in Figure 4C. These genes include ADRA1A, ADRA2C, ADRB1, DRD1, DRD3, GABRA2, GRIA1, GRM2, HTR1B, HTR1D, HTR2A, HTR2B, HTR7, and CHRNA7.

To further screen the 14 neurotransmitter-related receptor genes (NRGs) potentially targeted by XYS, we utilized publicly available human CRC transcriptomic data and clinical survival information from the TCGA and GEO databases.

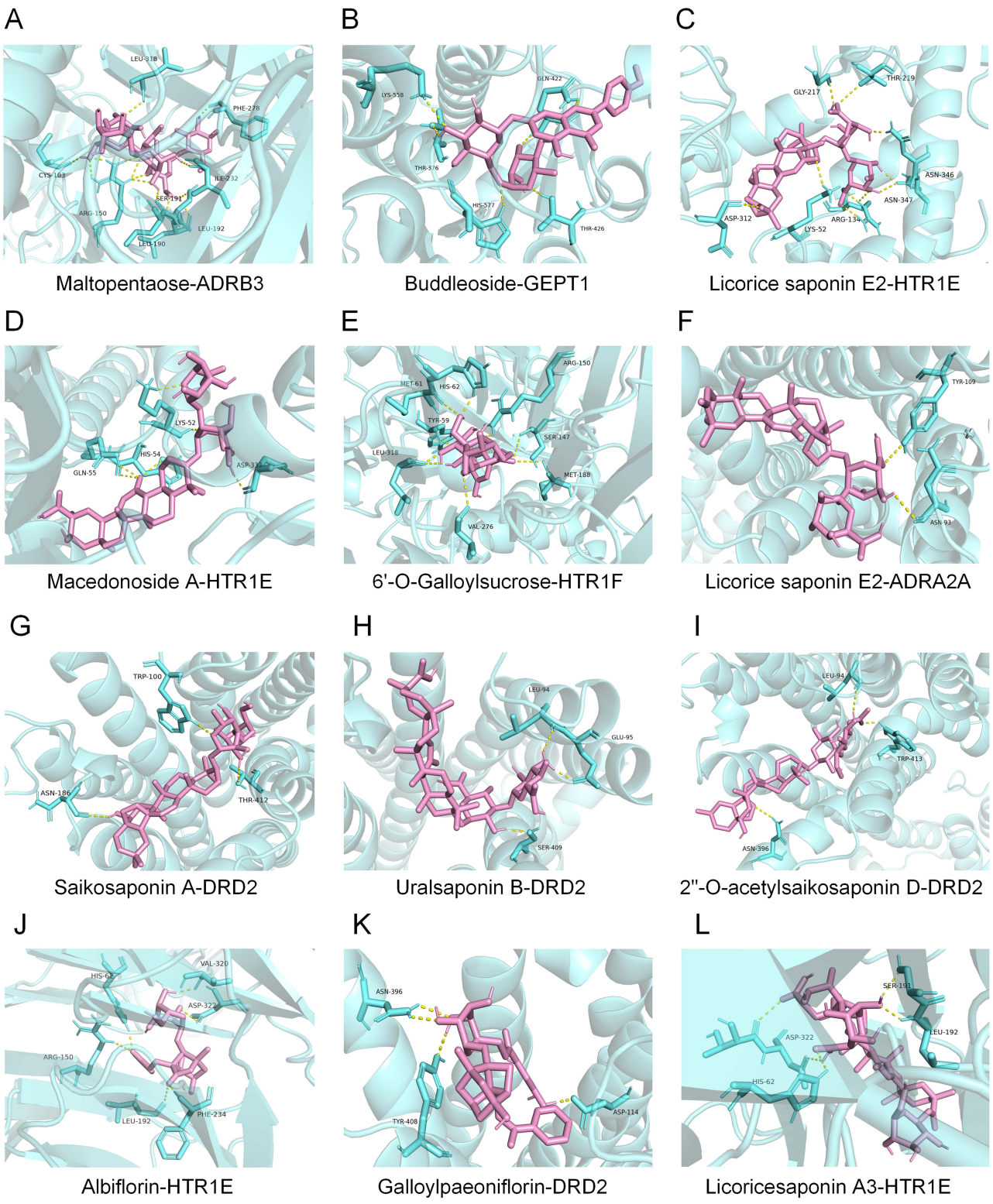

Figure 3 Molecular docking diagrams of XYS component ligands with their corresponding NRGs receptors. (**A**–**L**), in the diagrams, blue represents the receptors, pink represents the herbal small molecule compounds, and yellow dashed lines represent hydrogen bonds between the ligands and receptors. Each diagram labels the binding sites with "letter-number" combinations such as "LEU-318".

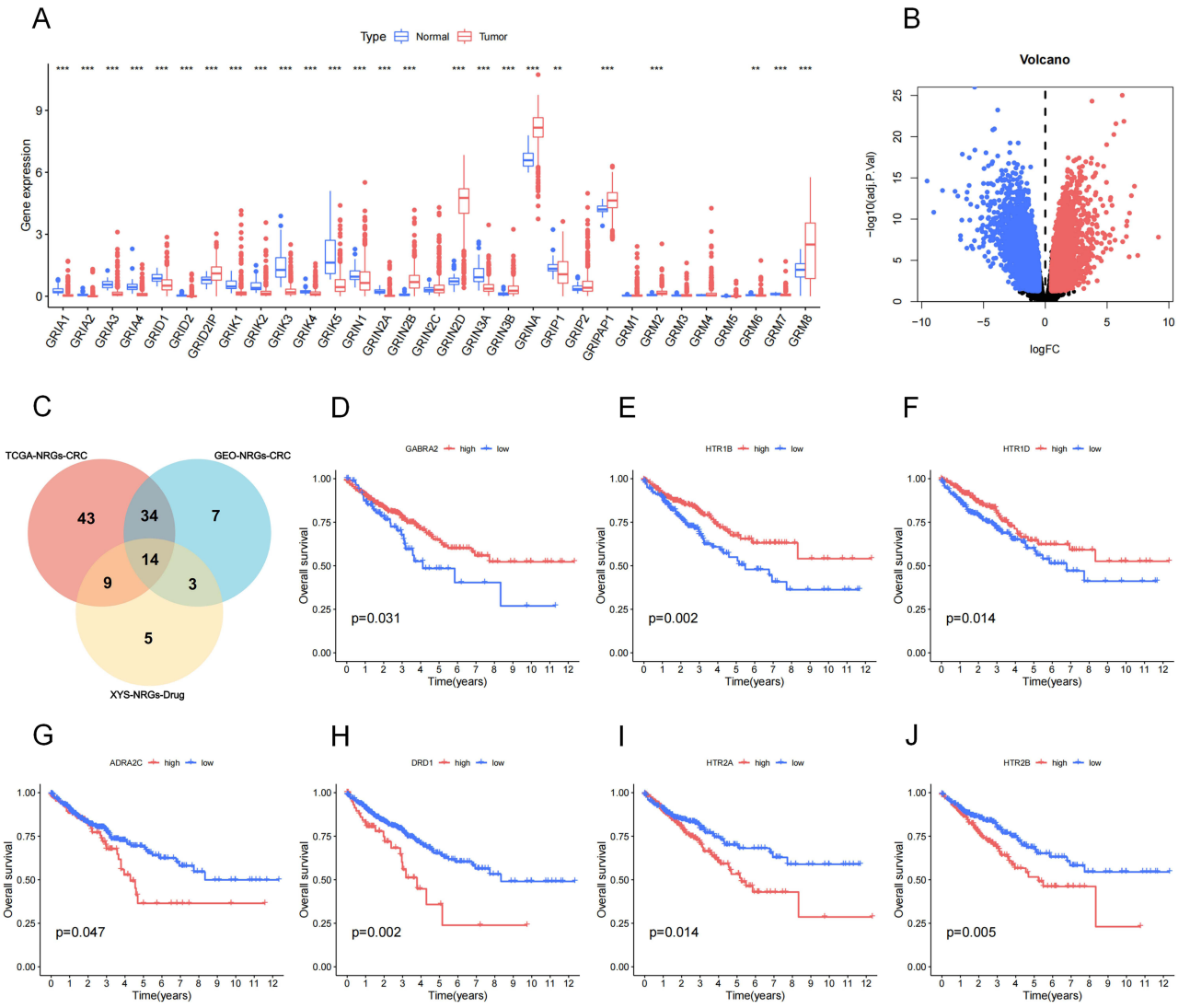

Figure 4 Screening of key NRGs targeted by XYS using TCGA and GEO databases. (**A**) shows the box plots of differential expression of Glu-related receptor genes in TCGA-CRC patients. Blue indicates reduced expression in tumor tissues, while red suggests increased expression (* for *P* value < 0.05, ** for *P* value < 0.01, *** for *P* value < 0.001). Box plots for the differential expression of other neurotransmitter receptors are shown in SFigure 1A–D. (**B**) shows presents the volcano plot of differentially expressed genes from the GEO dataset. (**C**)The Venn diagram of NRG intersection of NRG and XYS differentially expressed in CRC samples in TCGA and geo databases. (**D–J**) display the Kaplan-Meier survival curves for the hub-NRGs identified from the intersection of genes significantly associated with clinical patient prognosis.

Univariate COX regression analysis was performed to assess whether each NRG exhibited a significant association with the survival prognosis of CRC patients. This analysis revealed seven hub-NRGs significantly associated with clinical outcomes in CRC patients: ADRA2C, DRD1, GABRA2, HTR1B, HTR1D, HTR2A, and HTR2B. The survival curves for these genes are presented in Figure 4D–J. Among these, high expression levels of GABRA2, HTR1B, and HTR1D were associated with favorable clinical outcomes, whereas high expression levels of ADRA2C, DRD1, HTR2A, and HTR2B were correlated with poorer survival outcomes in CRC patients.

Excluding GABRA2, we compiled and plotted the molecular docking patterns for the remaining six NRGs significantly associated with clinical prognosis and their corresponding herbal compounds, as shown in Table 2 and Figure 5. Upon analyzing the docking results, we found that XYS's action on key NRGs in CRC is primarily mediated by the compounds 8-Debenzoylpaeoniflorin, Sucrose, and Tryptophan within the formula. Among these, 8-Debenzoylpaeoniflorin sourced from BS exhibited extensive and favorable binding capabilities, as depicted in Figure 5. According to Table 2, we identified that 8-Debenzoylpaeoniflorin mainly interacts with receptors related to neurotransmitters 5-HT, NE, and DA.

https://doi.org/10.2147/CMAR.S567746

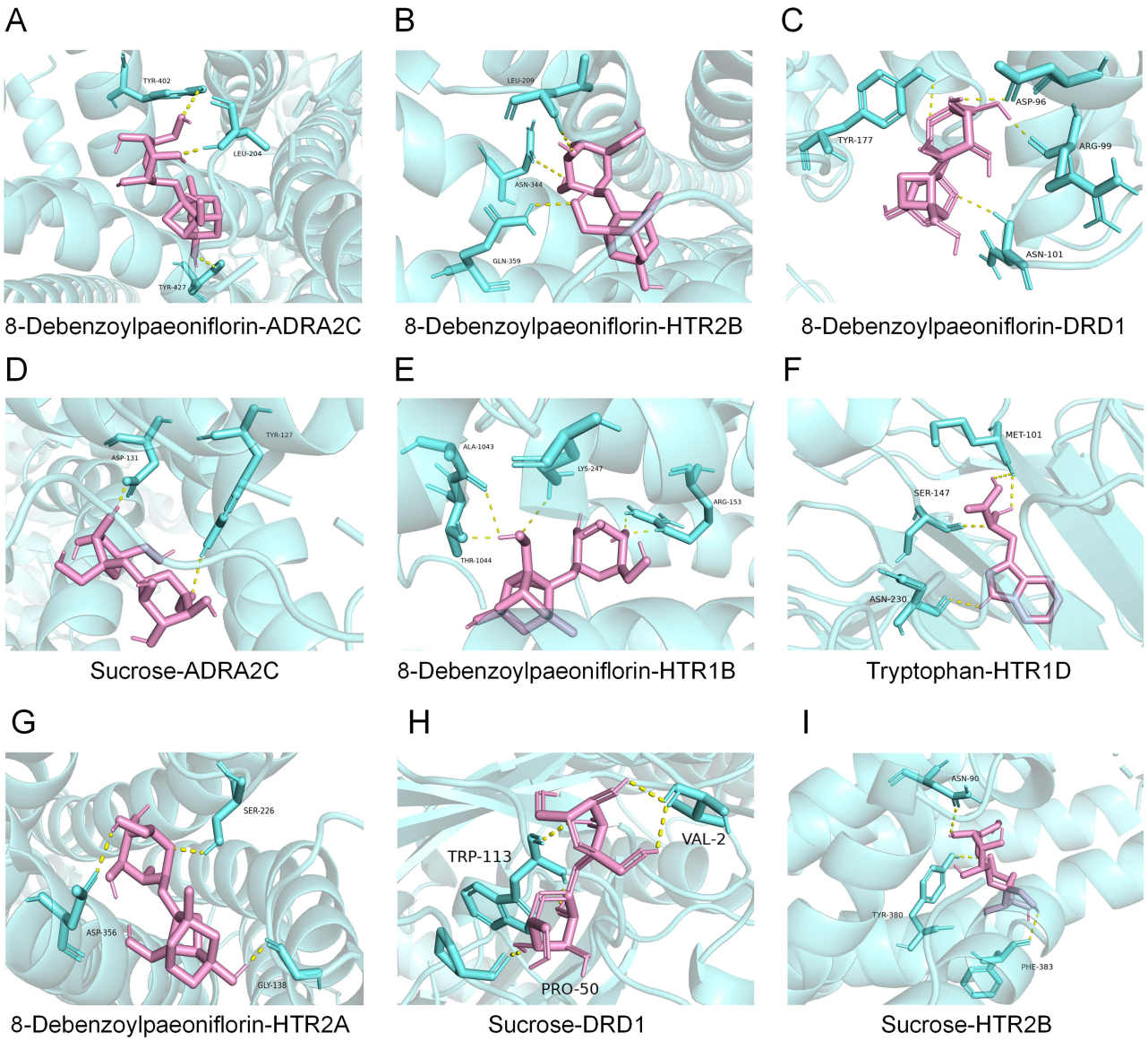

Figure 5 Molecular docking diagrams of the primary effective components of XYS with clinically significant hub-NRGs. (**A-I**) In the diagrams, blue represents the clinically significant hub-NRGs receptors, pink represents the corresponding XYS compound ligands, and yellow dashed lines represent hydrogen bonds between the ligands and receptors. Each diagram labels the binding sites with "letter-number" combinations such as "TYR-402.".

XYS Effectively Ameliorates Chronic Stress in Mice

Tumor anatomical photographs and line graphs of volume dynamics (Figure 6A and B) revealed that, compared with the control and model groups, intervention with XYS or fluoxetine significantly reduced tumor volume in mice. These findings suggest that antidepressant agents (XYS or fluoxetine) can alleviate tumor progression in stress-exposed mice. Regarding immune function modulation, assessments of spleen size and spleen index indicated that antidepressant interventions did not exert significant effects on overall immune activation in mice. Nevertheless, they still demonstrated the capacity to counteract chronic stress-induced immune suppression (Figure 6C and D). In terms of behavioral tests, results from the TST, FST, and OFT showed that XYS significantly ameliorated the chronic stress state in model mice, preserved their behavioral activity, and exhibited slightly superior efficacy compared to FXT (Figure 6E–G).

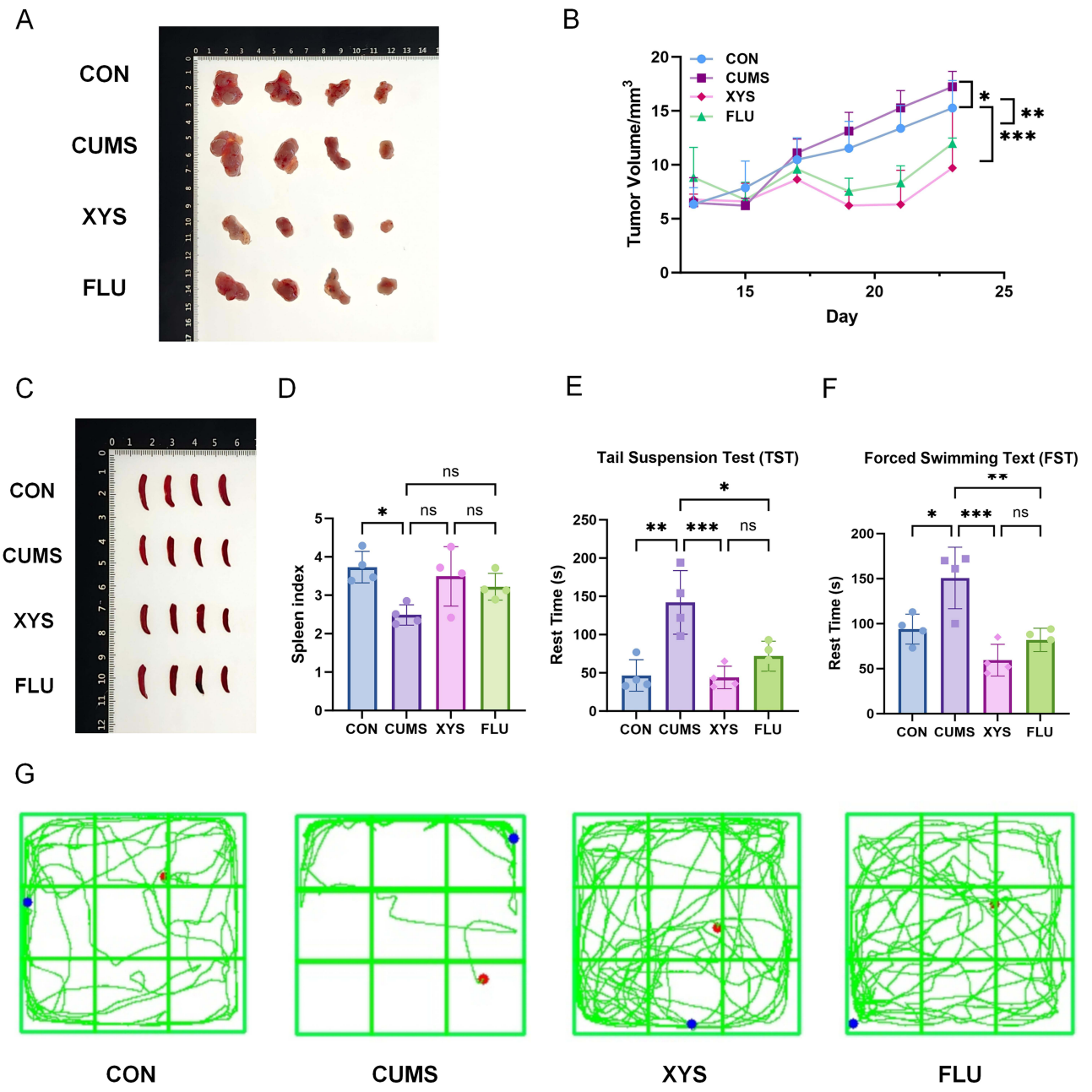

Figure 6 Effects of XYS on chronic stress, tumor progression, and immune function in mice. (**A**) Anatomical images of mouse tumors; (**B**) Line graph showing changes in mouse tumor volume over time; (**C**) Anatomical images of mouse spleens; (**D**) Bar chart of the spleen index; (**E** and **F**) Bar charts showing the results of the TST and FST, represented as immobility time. Typically, a longer immobility time indicates reduced locomotor activity and a state of chronic stress in the mice; (**G**) Track plots of mouse movement in the OFT. Greater total distance traveled and more frequent entries into the center zone are indicative of higher locomotor activity, whereas the opposite (ie, less distance traveled and fewer center entries) indicates lower activity and a state of chronic stress. (* for *P* value < 0.05, ** for *P* value < 0.01, *** for *P* value < 0.001, ns for *P* value >0.05).

Neurotransmitter Levels in Colorectal Cancer Mice with Chronic Stress Regulated by XYS

Mass spectrometry analysis was performed to measure the levels of major neurotransmitters in tumor tissues and plasma from mice in each group. The results showed that compared to the control group, the levels of 5-HT and DA in the tumor tissues of the CUMS group were significantly reduced, as shown in Figure 7A–C. However, these decreases in 5-HT levels under chronic stress were significantly reversed after XYS or FXT intervention. Similar trends were observed for

https://doi.org/10.2147/CMAR.S567746

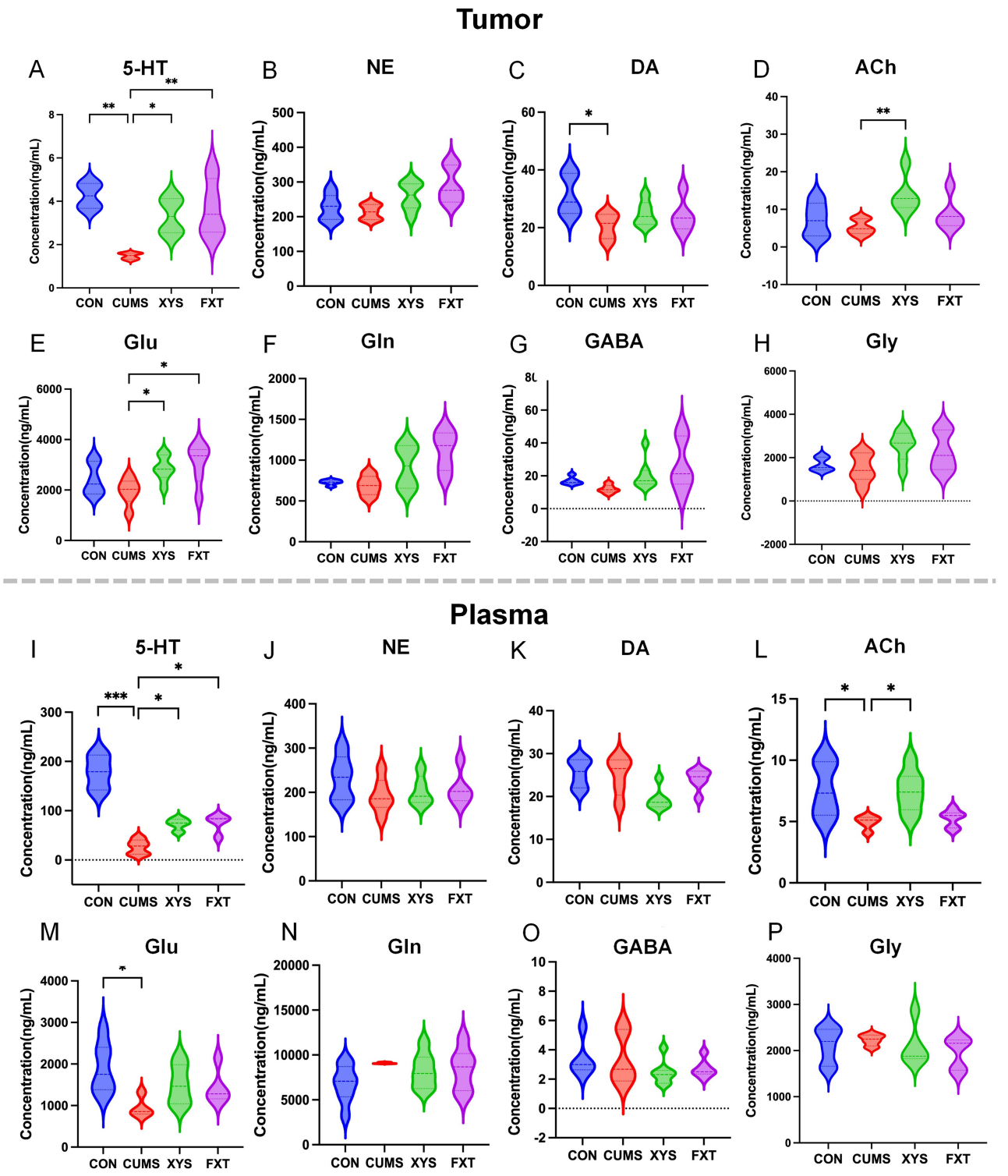

Figure 7 Variations in Neurotransmitter Levels Detected by Mass Spectrometry in Tumor Tissues and Plasma of Laboratory Model Mice. (**A**–**H**) The differences in major neurotransmitters in tumor tissues of each group were described, (**I**–**P**) The differences in major neurotransmitters in plasma between the groups (CON: tumor group, CUMS: chronic stress group, XYS: Xiao Yao San group, FXT: Fluoxetine group; * for *P* value < 0.05, ** for *P* value < 0.01, *** for *P* value < 0.001).

https://doi.org/10.2147/CMAR.S567746

ACh and Glu, although the reductions in ACh and Glu levels in the CUMS group did not reach statistical significance compared to the control group, possibly due to insufficient sample size. Nonetheless, a noticeable downward trend in the levels of these neurotransmitters was observed in the tumor tissues of the CUMS group, and this trend was significantly improved after XYS treatment, as shown in Figure 7D and E.

The results from plasma neurotransmitter detection provided additional insights. First, the plasma 5-HT levels followed the same trend as those in the tumor tissues, but the depletion of 5-HT in the plasma of the CUMS group was particularly pronounced, as shown in Figure 7I. Furthermore, the plasma levels of Glu and ACh were also significantly reduced under chronic stress, and these reductions were significantly ameliorated after XYS intervention, as shown in Figure 7L and M. Notably, the results from both tumor and plasma samples suggested that XYS exhibited superior efficacy in restoring ACh levels reduced by chronic stress. According to the previous network pharmacology results, this improvement may be associated with the targeting of the ACh receptor CHRNA7.

Single-Cell Sequencing Analysis of Immune Cell Alterations in the Tumor Microenvironment

To further confirm the effects of chronic stress and XYS on immune cells in the CRC TME, we employed single-cell sequencing to detect differential changes in immune cells within the TME, as shown in Figure 8A. Following quality control and dimensionality reduction-based clustering, a total of 14 distinct cell types were identified from the mouse tumor tissues. The distribution of these cell types across the control, CUMS, and XYS groups is illustrated in Figures 8B–D. Notably, the

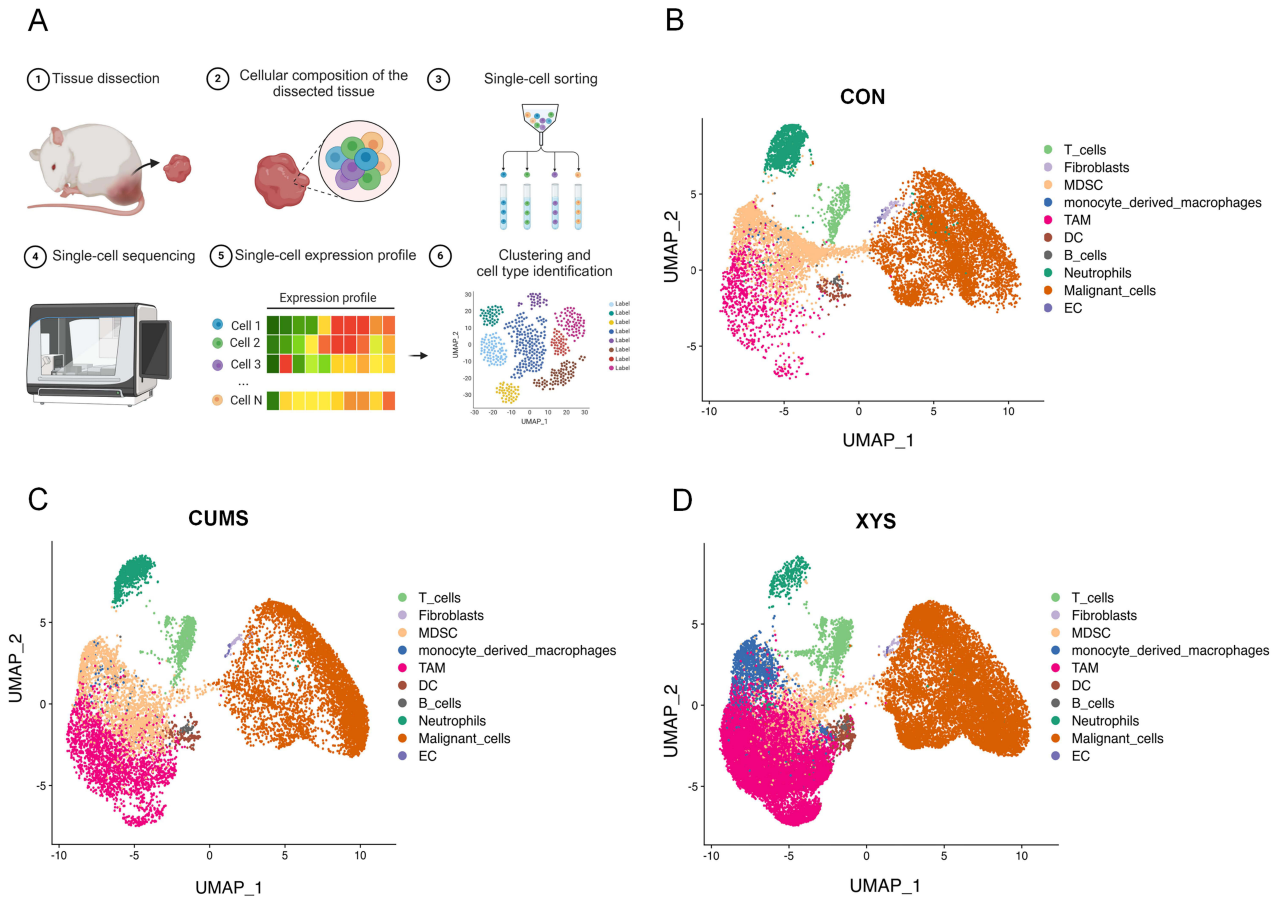

Figure 8 Single-Cell Sequencing Workflow and Clustering Diagram. (**A**) Workflow of single-cell sequencing; (**B**) Distribution of clustered cells in the CON group; (**C**) Distribution of clustered cells in the CUMS group; (**D**) Distribution of clustered cells in the XYS group. The horizontal and vertical axes represent the first and second principal components of dimensionality reduction, respectively, with different cell clusters differentiated by distinct colors.

https://doi.org/10.2147/CMAR.S567746

cluster distribution plots revealed an increased abundance of myeloid-derived suppressor cells (MDSCs) in the CUMS group compared to the control group, while treatment with XYS resulted in a reduction of MDSCs.

In our previous study, we identified neurotransmitters NE, DA, and 5-HT as potentially key mediators through which chronic stress influences CRC progression. Therefore, when analyzing differentially expressed NRGs across immune cell subsets, we paid particular attention to the expression of receptors for these three neurotransmitters, as shown in Figure 9 and Supplementary Figure 2. We observed that in dendritic cells (DCs), the expression of *Adrb2* in the XYS group differed significantly from that in the CUMS group (Figure 9A). In malignant cells, the expression levels of *Drd1, Htr2a*,

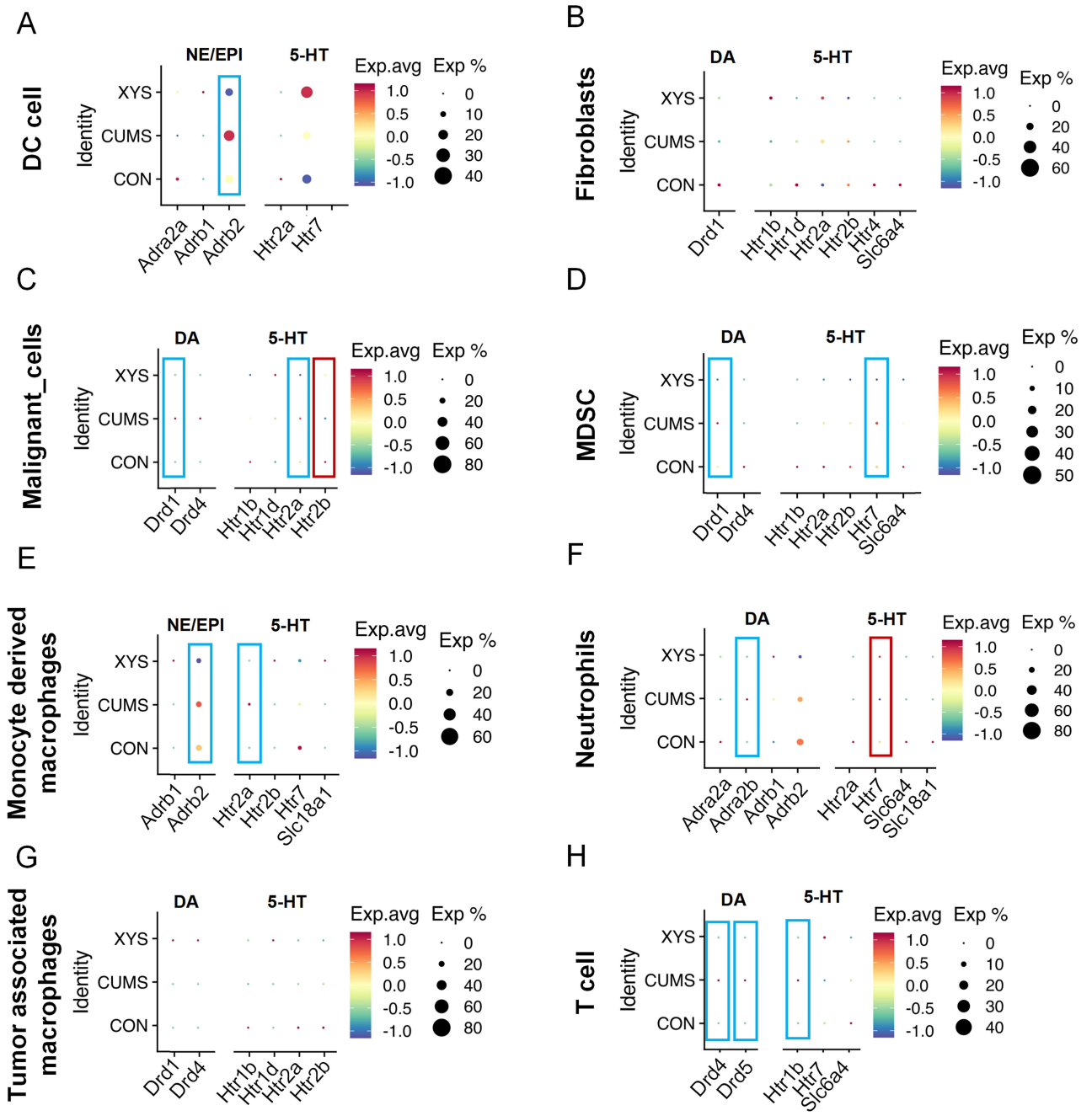

Figure 9 Immune Cell Receptor Gene Expression Bubble Charts of NRGs. The bubble charts in (**A**–**H**) represent the differential expression of hub-NRGs among the three groups of samples in these immune cells. Based on the previous results, this figure only displays differential expression of NEGs related to NE/EPI, DA, and 5-HT. For complete results, please refer to Figure S2 and 3. Blue boxes indicate a decrease in receptor expression in the XYS group compared to CUMS group in these immune cells, while red boxes indicate an increase in receptor expression compared to CUMS group in these immune cells.

https://doi.org/10.2147/CMAR.S567746

and *Htr2b* in the XYS group aligned with the expression trend seen in the CON group (Figure 9C). In MDSCs, *Drd1* expression was markedly increased in the CUMS group but was significantly suppressed following XYS administration (Figure 9D). In neutrophils, the elevated expression of *Adra2a* and *Htr1b* induced by CUMS was reversed after XYS intervention (Figure 9F). Moreover, in monocyte-derived macrophages and T cells, XYS treatment restored the CUMS-induced overexpression of *Htr2a* and *Htr1b* to levels comparable to those in the control group (Figure 9E and H, respectively). These findings indicate that XYS can modulate the expression of NRGs in immune cells.

To further investigate the relevance of XYS-regulated NRGs and their corresponding immune cells in human CRC, we utilized the Timer 2.0 database for correlation analysis. The database revealed that DRD1 did not show a significant correlation with MDSCs in CRC, as shown in SFigure 3A. In contrast, HTR2A exhibited a predominantly positive correlation with macrophages in both colon adenocarcinoma (COAD) and rectal adenocarcinoma (READ), as demonstrated in SFigure 3B and Figure 10A. Furthermore, CIBERSORT-ABS analysis indicated that HTR1B was positively correlated with $CD8^+$ T cells, $CD4^+$ T cells, and Treg cells in both COAD and READ, as shown in Figure 10B and C.

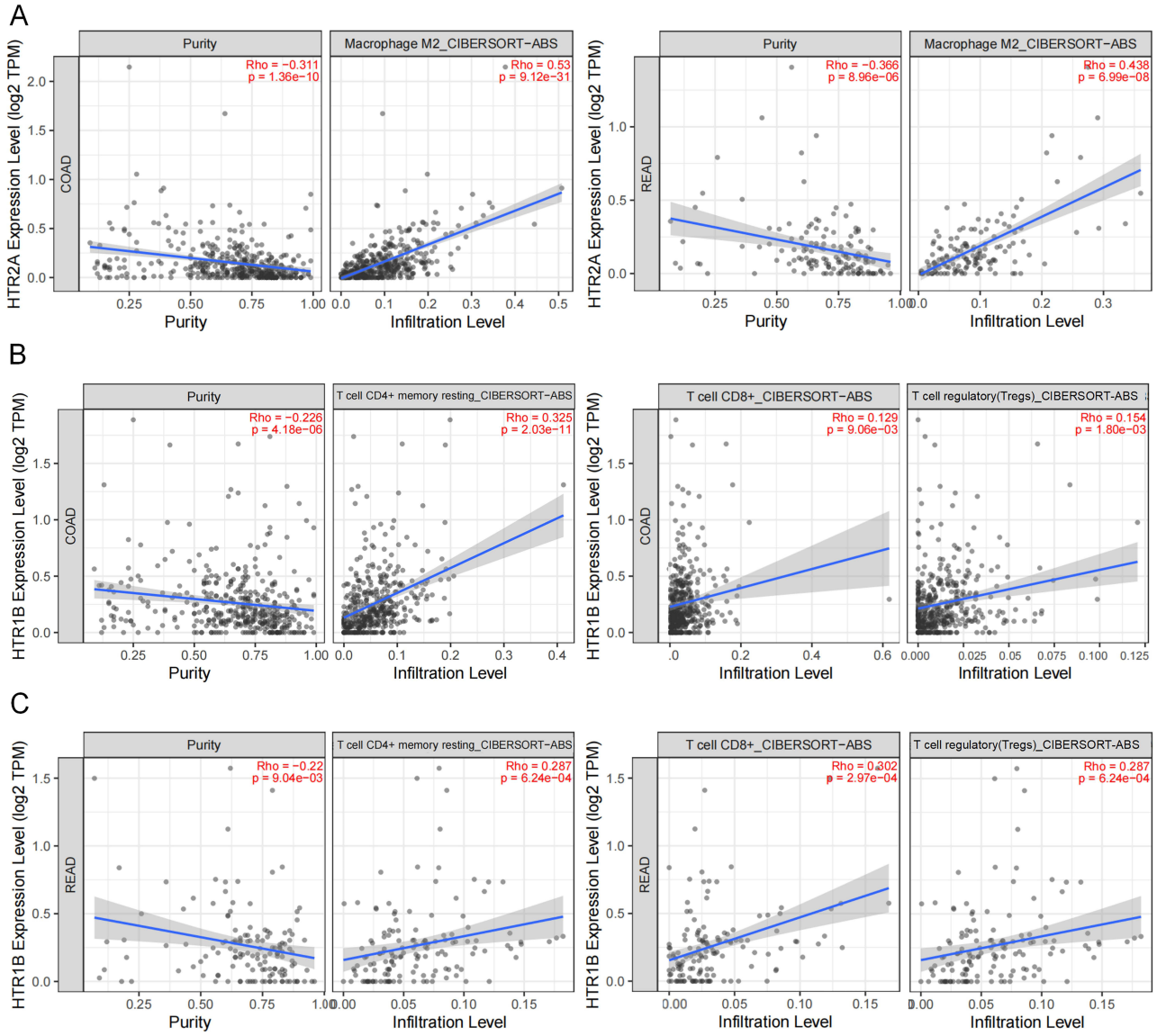

Figure 10 Scatter Plots of Correlations Between Key NRGs and Human CRC Immune Cells. (**A**) Scatter plots showing the correlation between HTR2A and macrophages in COAD and READ, respectively. (**B**) Scatter plots of the correlation between HTR1B and $CD4^+$ T cells, CD8+ T cells, and Treg cells in COAD. (**C**) Scatter plots of the correlation between HTR1B and $CD4^+$ T cells, CD8+ T cells, and Treg cells in READ. "Purity" is a major confounding factor in this analysis, typically used to indicate the estimate of infiltration, and most immune cell types show a negative correlation with tumor purity.

https://doi.org/10.2147/CMAR.S567746

Our single-cell analysis further revealed that, compared to the control group, CUMS stimulation increased the expression of HTR2A in macrophages and HTR1B in T cells within the CRC TME. This suggests that chronic stress exacerbates neuro-immune interactions in CRC. However, after XYS treatment, this elevated expression was suppressed, restoring the levels to those observed in the absence of chronic stress.

KEGG pathway enrichment analysis is a commonly used method in bioinformatics to screen potential mechanisms of action. By performing single-cell sequencing to identify differentially expressed genes (DEGs) among the groups and conducting KEGG pathway enrichment analysis based on these DEGs, we can explore the potential pathways through which CUMS and XYS exert their effects on CRC. Encouragingly, the KEGG functional analysis across the three groups also indicated that the activation and recruitment of the nervous and immune systems represent potential pathways underlying the effects of chronic stress and XYS, as shown in Figure 11A and B. These findings provide confidence for further in-depth exploration of how traditional Chinese compound medications modulate the neuro-immune axis to improve chronic stress and stress-exacerbated CRC mechanisms.

Discussion

Chronic stress is a common comorbidity in colorectal cancer (CRC) patients and significantly influences CRC progression.[5] Clinical studies have demonstrated that cancer patients with anxiety or depression often exhibit poorer clinical outcomes.[38] Many researchers attribute this phenomenon to stress-induced alterations in the tumor immune microenvironment.[39] Chronic stress can markedly change the levels of neurotransmitters such as ACh),[40] 5-HT, and NE.[41] These neurotransmitters directly regulate the functions of immune cells—including T cells, macrophages, and MDSCs—through their corresponding receptors (eg, β-AR, DRD, HTR), thereby forming a neuro-immune regulatory network.[42] For instance, chronic stress stimulates intestinal enterochromaffin cells to release excessive 5-HT, which triggers immune responses in mast cells, neutrophils, and monocytes via specific receptors, ultimately disrupting intestinal homeostasis.[43] In CRC, such neuro-immune interactions also play a crucial role. Our bioinformatics analysis revealed that multiple NRGs are significantly dysregulated in CRC patients and correlated with prognosis, suggesting that disturbances in the neurotransmitter system contribute to CRC progression. Previous studies have observed that chronic stress-induced upregulation of adrenergic receptors (eg, β-AR) is closely associated with accelerated tumor growth and metastasis.[44,45] Therefore, mitigating chronic stress represents an important aspect of CRC management.

TCM is rooted in the TCM syndrome differentiation system and employs combinations of natural herbal medicines to treat diseases. Extensive research indicates that Chinese herbal formulas exert multi-target and multi-pathway effects, particularly in managing cancer-related complications and psychological disorders. As a representative TCM formula for depression, XYS plays an indispensable role in clinical antidepressant therapy.[18] Long-term use of conventional antidepressants such as amitriptyline and FXT is often accompanied by side effects including nausea, vomiting, and anxiety.[46] In contrast, XYS achieves therapeutic effects comparable to those of conventional antidepressants while reducing the incidence of adverse reactions, thereby improving treatment compliance and overall quality of life.[47] Modern studies confirm that XYS significantly modulates neurotransmitter levels,[15] alleviates inflammatory responses in depression by regulating multiple metabolic pathways and targets,[22] exerts antidepressant effects by adjusting the levels of neurotransmitters such as 5-HT, DA, and NE and enhancing cation transporter expression,[18] and reinforces its antidepressant action by increasing the number and function of microglia and astrocytes and stimulating changes in 5-HT in vivo.[48,49] Moreover, XYS has also demonstrated notable efficacy in treating cancers such as breast cancer,[17] ovarian cancer,[50] and CRC.[51] Our previous work confirmed that XYS effectively improves CRC under chronic stress; however, whether this improvement is mediated through modulation of neurotransmitter levels and the neuro-immune axis remained unclear. To address this, we employed an integrated approach combining bioinformatics analysis, molecular docking, animal models, and single-cell sequencing to validate this hypothesis.

In this study, network pharmacology was applied to predict targets of the XYS components previously identified by UHPLC/Q-TOF-MS, yielding 1,228 potential drug targets. Through molecular docking between these drug targets and NRGs, we verified that XYS interacts with receptors for multiple neurotransmitters. By analyzing CRC patient samples and survival data from TCGA and GEO databases, univariate COX analysis identified seven hub NRGs: ADRA2C, DRD1, GABRA2, HTR1B, HTR1D, HTR2A, and HTR2B. Our results indicate that the regulation of receptors for

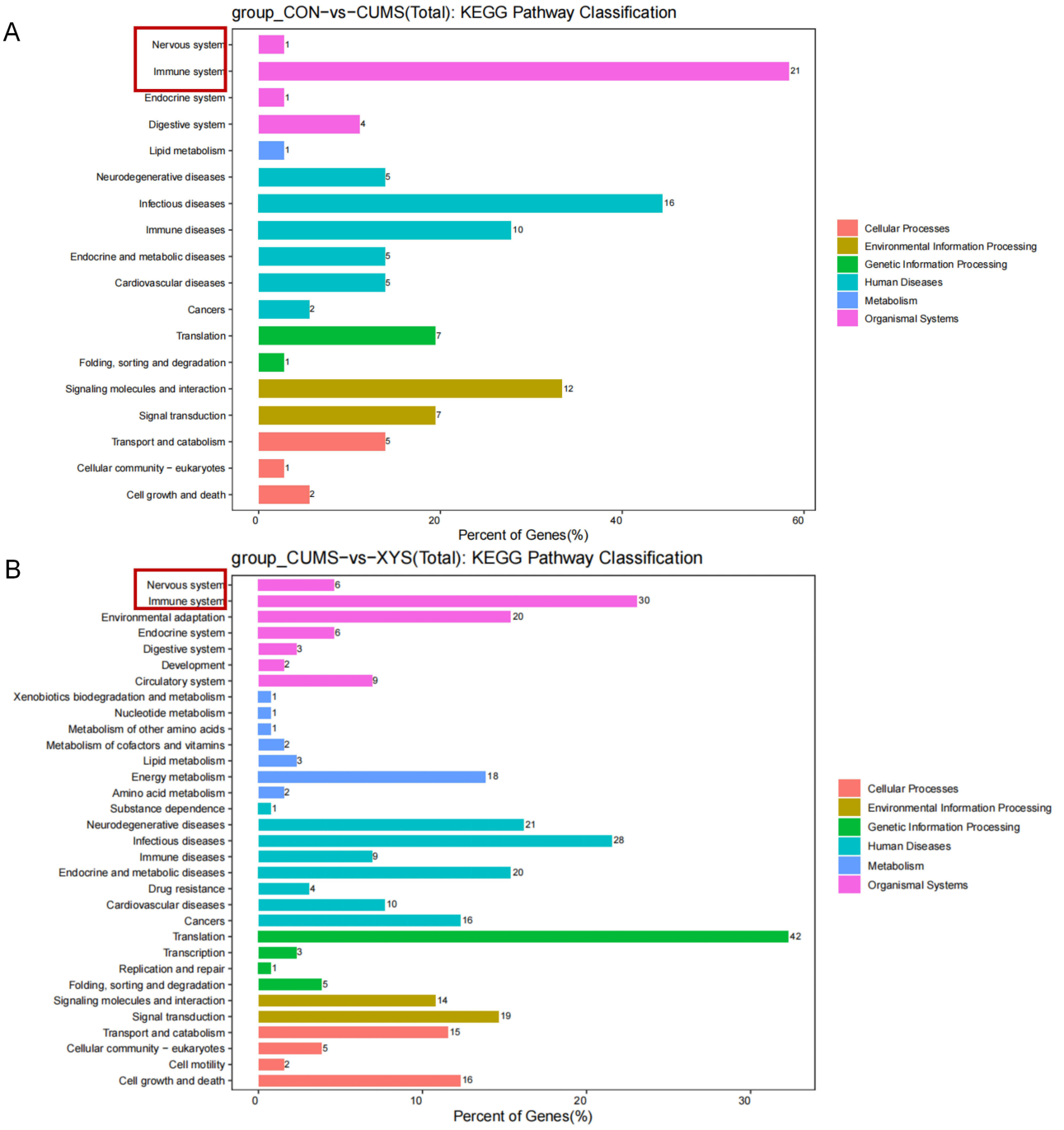

Figure 11 KEGG Pathway Enrichment Analysis. (**A**) KEGG pathway enrichment plot for the CON group versus the CUMS group; (**B**) KEGG pathway enrichment plot for the CUMS group versus the XYS group. The vertical axis represents the pathways enriched by differentially expressed genes, categorized into six classifications: Metabolism, Genetic Information Processing, Environmental Information Processing, Cellular Processes, Organismal Systems, and Human Diseases, indicated by different colors. The horizontal axis represents the ratio (%) of differentially expressed genes annotated to each classification pathway to the total number of differentially expressed genes annotated to all KEGG pathways. (The numbers in the bar graph represent the percentage of genes (%) enriched in each KEGG pathway classification).

neurotransmitters such as NE, DA, and 5-HT is key to the influence of XYS on CRC prognosis. Published studies have shown that CUMS-induced depression/anxiety-like behaviors are associated with significantly reduced mRNA expression of monoamine system receptors, including HTR2A, ADRB3, and ADRA2C, in the mouse hippocampus.[52] Accordingly, we established a CUMS mouse model and administered XYS and fluoxetine (positive control). Measurements of neurotransmitters and single-cell sequencing results corroborated that XYS indeed affects both

https://doi.org/10.2147/CMAR.S567746

neurotransmitter levels and immune cells in CRC under chronic stress, suggesting that XYS may simultaneously exert antidepressant and anti-tumor effects.

Notably, our findings revealed that 8-Debenzoylpaeoniflorin from *Paeonia lactiflora* exhibits broad and strong binding affinity to neurotransmitter-related receptors. 8-Debenzoylpaeoniflorin is generally regarded as a metabolite of paeoniflorin.[53] In studies on *Paeonia lactiflora* or formulas containing it, such as Dang-Gui-Shao-Yao-San, 8-Debenzoylpaeoniflorin has been detected at significant levels in the plasma of herb-treated rats,[54] indicating good oral bioavailability. This suggests that 8-Debenzoylpaeoniflorin may be one of the key components through which XYS regulates the neurotransmitter system.

In animal experiments, XYS significantly improved CUMS-induced depression-like behaviors and suppressed tumor growth. Mass spectrometry further demonstrated that XYS reversed the abnormal levels of NE, DA, and 5-HT in both tumor tissue and plasma induced by chronic stress. These results suggest that XYS not only exerts antidepressant effects but also restores neurotransmitter homeostasis locally in the tumor and systemically.

Using scRNA-seq technology, we dissected the impact of XYS on immune cells in the tumor microenvironment at single-cell resolution. The results showed that chronic stress significantly increased the proportion of MDSCs and up-regulated the expression of HTR2A in macrophages and HTR1B in T cells. XYS intervention reversed these changes, restoring immune cell subset proportions and NRG expression toward normal levels. This high-resolution evidence confirms that XYS can counteract chronic stress-induced immunosuppression by modulating neurotransmitter receptor expression in specific immune cell subsets.

This study has several limitations. First, although molecular docking predicted interactions between XYS components and NRGs, further in vitro binding assays and signaling pathway validation are needed. Second, while animal models simulate chronic stress and tumor progression, the neuro-immune regulatory network in mice differs from that in humans. Future studies could employ organoid or humanized mouse models to further validate the regulatory mechanisms of XYS in human settings.

Conclusions

This study elucidates that XYS ameliorates chronic stress-induced colorectal cancer progression by regulating key neurotransmitter receptor genes (eg, HTR1B, DRD1, HTR2A). XYS exerts multi-target holistic effects in restoring neurotransmitter homeostasis and reversing immunosuppression in the tumor microenvironment—such as reducing MDSC proportion and modulating NRG expression in macrophages and T cells. Compared with conventional antidepressants, XYS demonstrates multi-pathway synergistic advantages in regulating the neuro-immune axis, offering a potential integrated intervention strategy for the clinical management of CRC patients with comorbid emotional disorders.

Abbreviations

ACh, Acetylcholine; CRC, colorectal cancer; GABA, γ-Aminobutyric Acid; COAD, colon cancer; DA, Dopamine; ENS, enteric nervous system; GEO, gene expression omnibus; Glu, Glutamate; HPA axis, hypothalamic-pituitary-adrenal axis; OFT, open field test; NRGs, neurotransmitter-related receptor genes; SAM axis, sympathetic-adrenal medullary axis; TCGA, The cancer genome atlas; TME, tumor microenvironment; TST, tail suspension test; FST, forced swim test; SPT, sucrose preference test; MNN, Mutual Nearest Neighbors; UMAP, Uniform Manifold Approximation and Projection; SNN, Shared Nearest Neighbors; EPI, Epinephrine; NE, Norepinephrine; READ, rectal cancer; TCM, Traditional Chinese Medicine. XYS, Xiao-yao-san; 5-HT, 5-hydroxytryptamine.

Data Sharing Statement

The single-cell sequencing data used in this study have been uploaded to the Gene Expression Omnibus (GEO) database under the accession number GSE275178. The dataset is under continuous update according to the content of the authors' research.

Ethics Approval and Informed Consent

This research, using publicly available data is exempt from ethical approval under item 1 and 2 of Article 32 of the Measures for Ethical Review of Life Science and Medical Research Involving Human Subjects dated February 18, 2023, China. The animal experiment plan conforms to the executive standard of the national code for the use of experimental

animals (China) and was approved by the ethics committee of the Shanghai University of Traditional Chinese Medicine (pzshutcm220913004).

Author Contributions

YL: Writing – original draft, Formal analysis, Validation, Visualization, Data curation, Conceptualization, investigantion. SY Y: Writing – review & editing, Formal analysis, Validation, investigantion. HR L and YC S: Validation, Data curation. HC L and XY H: Validation, Data curation. YR Z: Conceptualization, Data curation, Validation, Investigation, Project administration, Supervision. YW: Resources, Funding acquisition, Conceptualization.

Funding

This work was supported by the Science Foundation of China (82474230), Postdoctoral Fellowship Program of CPSF under Grant Number GZB20250914, Natural Science Foundation of Shanghai (25ZR1402484), Special Funds for High-level Creative Talents Cultivation in Guizhou Province [Qian Ke He XKBF (2025) 027; XKBF (2025) 028)], open foundation of Chinese Medicine Guangdong Laboratory (HQL2025OPA016).

Disclosure

The author(s) report no conflicts of interest in this work.

References

1. Laskar RS, Qu C, Huyghe JR, et al. Genome-wide association studies and Mendelian randomization analyses provide insights into the causes of early-onset colorectal cancer. *Ann Oncol*. 2024;35(6):523–536. doi:10.1016/j.annonc.2024.02.008
2. Murphy CC, Zaki TA. Changing epidemiology of colorectal cancer — birth cohort effects and emerging risk factors. *Nat Rev Gastroenterol Hepatol*. 2024;21(1):25–34. doi:10.1038/s41575-023-00841-9
3. Hartung TJ, Brähler E, Faller H, et al. The risk of being depressed is significantly higher in cancer patients than in the general population: prevalence and severity of depressive symptoms across major cancer types. *Eur J Cancer*. 2017;72:46–53. doi:10.1016/j.ejca.2016.11.017
4. Bertocchi A, Carloni S, Ravenda PS, et al. Gut vascular barrier impairment leads to intestinal bacteria dissemination and colorectal cancer metastasis to liver. *Cancer Cell*. 2021;39(5):708–724.e711. doi:10.1016/j.ccell.2021.03.004
5. McCollum SE, Shah YM. Stressing out cancer: chronic stress induces dysbiosis and enhances colon cancer growth. *Cancer Res*. 2024;84 (5):645–647. doi:10.1158/0008-5472.CAN-23-3871
6. Xu MY, Guo CC, Li MY, et al. Brain-gut-liver axis: chronic psychological stress promotes liver injury and fibrosis via gut in rats. *Front Cell Infect Microbiol*. 2022;12:1040749. doi:10.3389/fcimb.2022.1040749
7. Qiao G, Chen M, Mohammadpour H, et al. Chronic adrenergic stress contributes to metabolic dysfunction and an exhausted phenotype in T cells in the tumor microenvironment. *Cancer Immunol Res*. 2021;9(6):651–664. doi:10.1158/2326-6066.CIR-20-0445
8. Yang J, Wei W, Zhang S, Jiang W. Chronic stress influences the macrophage M1-M2 polarization balance through β-adrenergic signaling in hepatoma mice. *Int Immunopharmacol*. 2024;138:112568. doi:10.1016/j.intimp.2024.112568
9. Shao S, Jia R, Zhao L, et al. Xiao-Chai-Hu-Tang ameliorates tumor growth in cancer comorbid depressive symptoms via modulating gut microbiota-mediated TLR4/MyD88/NF-κB signaling pathway. *Phytomedicine*. 2021;88:153606. doi:10.1016/j.phymed.2021.153606
10. Sacristán C. Partners and guardians of the nervous and immune systems. *Trends in Immunol*. 2024;45(5):315–317. doi:10.1016/j.it.2024.04.007
11. Ma Y, Kroemer G. The cancer-immune dialogue in the context of stress. *Nat Rev Immunol*. 2024;24(4):264–281. doi:10.1038/s41577-023-00949-8
12. Zhang Y, Wang Y. The dual roles of serotonin in antitumor immunity. *Pharmacol Res*. 2024;205:107255. doi:10.1016/j.phrs.2024.107255
13. Yang S, Li Y, Zhang Y, Wang Y. Impact of chronic stress on intestinal mucosal immunity in colorectal cancer progression. *Cytokine Growth Factor Rev*. 2024;80:24–36. doi:10.1016/j.cytogfr.2024.10.007
14. Zhang Y, Feng Y, Zhao Y, et al. Single-cell RNA sequencing reveals that the immunosuppression landscape induced by chronic stress promotes colorectal cancer metastasis. *Heliyon*. 2024;10(1):e23552. doi:10.1016/j.heliyon.2023.e23552
15. Wang YT, Wang XL, Wang ZZ, Lei L, Hu D, Zhang Y. Antidepressant effects of the traditional Chinese herbal formula Xiao-Yao-San and its bioactive ingredients. *Phytomedicine*. 2023;109:154558. doi:10.1016/j.phymed.2022.154558
16. Wang Y, Chen X, Wei W, et al. Efficacy and safety of the Chinese herbal medicine Xiao Yao San for treating anxiety: a systematic review with meta-analysis and trial sequential analysis. *Front Pharmacol*. 2023;14:1169292. doi:10.3389/fphar.2023.1169292
17. Pan J, Fu S, Zhou Q, Lin D, Chen Q. Modified xiaoyao san combined with chemotherapy for breast cancer: a systematic review and meta-analysis of randomized controlled trials. *Front Oncol*. 2023;13:1050337. doi:10.3389/fonc.2023.1050337
18. Wu Y, Liu L, Zhao Y, et al. Xiaoyaosan promotes neurotransmitter transmission and alleviates CUMS-induced depression by regulating the expression of Oct1 and Oct3 in astrocytes of the prefrontal cortex. *J Ethnopharmacol*. 2024;326:117923. doi:10.1016/j.jep.2024.117923
19. Kwon T-G, Kim Y-J, Hong J-Y, Song J-H, Park J-Y. A review of antidepressant and anxiolytic effects of Soyo-san (Xiaoyao-san) and modified Soyo-san in animal models. *Phytomedicine*. 2024;135:155387. doi:10.1016/j.phymed.2024.155387
20. Chen WF, Xu L, Yu CH, et al. The in vivo therapeutic effect of free wanderer powder (xiāo yáo sǎn, Xiaoyaosan) on mice with 4T1 cell induced breast cancer model. *J Traditional Complementary Med*. 2012;2(1):67–75. doi:10.1016/s2225-4110(16)30073-6
21. Meng P, Zhang X, Liu TT, et al. A whole transcriptome profiling analysis for antidepressant mechanism of Xiaoyaosan mediated synapse loss via BDNF/trkB/PI3K signal axis in CUMS rats. *BMC Complement Med Therap*. 2023;23(1):198. doi:10.1186/s12906-023-04000-0

22. Zhang Y, Li XJ, Wang XR, et al. Integrating metabolomics and network pharmacology to explore the mechanism of Xiao-Yao-San in the treatment of inflammatory response in CUMS mice. *Pharmaceuticals*. 2023;16(11).
23. Cao GP, Gui D, Fu LD, Guo ZK, Fu WJ. Anxiolytic and neuroprotective effects of the traditional Chinese medicinal formulation Dan-zhi-xiao-yao-san in a rat model of chronic stress. *Mole Med Reports*. 2016;14(2):1247–1254. doi:10.3892/mmr.2016.5382
24. Ding F, Wu J, Liu C, et al. Effect of Xiaoyaosan on colon morphology and intestinal permeability in rats with chronic unpredictable mild stress. *Front Pharmacol*. 2020;11:1069. doi:10.3389/fphar.2020.01069
25. Ji S, Han S, Yu L, et al. Jia Wei Xiao Yao San ameliorates chronic stress-induced depression-like behaviors in mice by regulating the gut microbiome and brain metabolome in relation to purine metabolism. *Phytomedicine*. 2022;98:153940. doi:10.1016/j.phymed.2022.153940
26. Liu X, Liu H, Wu X, et al. Xiaoyaosan against depression through suppressing LPS mediated TLR4/NLRP3 signaling pathway in "microbiota-gut-brain" axis. *J Ethnopharmacol*. 2024;335:118683. doi:10.1016/j.jep.2024.118683
27. Chen J, Lei C, Li X, et al. Research progress on classical traditional Chinese medicine formula xiaoyaosan in the treatment of depression. *Front Pharmacol*. 2022;13:925514. doi:10.3389/fphar.2022.925514
28. Jiao H, Fan Y, Gong A, Li T, Fu X, Yan Z. Xiaoyaosan ameliorates CUMS-induced depressive-like and anorexia behaviors in mice via necroptosis related cellular senescence in hypothalamus. *J Ethnopharmacol*. 2024;318(Pt A):116938. doi:10.1016/j.jep.2023.116938
29. Jing LL, Zhu XX, Lv ZP, Sun X-G. Effect of Xiaoyaosan on major depressive disorder. *ChinMed*. 2015;10(1):18. doi:10.1186/s13020-015-0050-0
30. Zhang Z, Shao S, Zhang Y, et al. Xiaoyaosan slows cancer progression and ameliorates gut dysbiosis in mice with chronic restraint stress and colorectal cancer xenografts. *Biomed Pharmacothe*. 2020;132:110916.
31. Shao S, Zhang Z, Zhang Y, et al. A method to establish a chronic restraint stress mouse model with colorectal cancer xenografts. *MethodsX*. 2021;8:101304. doi:10.1016/j.mex.2021.101304
32. Liu MY, Yin CY, Zhu LJ, et al. Sucrose preference test for measurement of stress-induced anhedonia in mice. *Nat Protoc*. 2018;13(7):1686–1698. doi:10.1038/s41596-018-0011-z
33. Song AQ, Gao B, Fan JJ, et al. NLRP1 inflammasome contributes to chronic stress-induced depressive-like behaviors in mice. *J Neuroinflammation*. 2020;17(1):178. doi:10.1186/s12974-020-01848-8
34. Chang SN, Kang SC. Decursinol angelate inhibits glutamate dehydrogenase 1 activity and induces intrinsic apoptosis in MDR-CRC cells. *Cancers*. 2023;15(14). doi:10.3390/cancers15143541
35. Wang H, Zhang H, Sun Z, Chen W, Miao C. GABAB receptor inhibits tumor progression and epithelial-mesenchymal transition via the regulation of Hippo/YAP1 pathway in colorectal cancer. *Int J Bio Sci*. 2021;17(8):1953–1962. doi:10.7150/ijbs.58135
36. Terasaki M, Mima M, Kudoh S, et al. Glycine and succinic acid are effective indicators of the suppression of epithelial-mesenchymal transition by fucoxanthinol in colorectal cancer stem-like cells. *Oncol Rep*. 2018;40(1):414–424. doi:10.3892/or.2018.6398
37. Schirmer B, Rother T, Bruesch I, et al. Genetic deficiency of the histamine H(4)-receptor reduces experimental colorectal carcinogenesis in mice. *Cancers*. 2020;12(4):912. doi:10.3390/cancers12040912
38. Takvorian SU, Gabriel P, Wileyto EP, et al. Clinician- and patient-directed communication strategies for patients with cancer at high mortality risk: a cluster randomized trial. *JAMA Network Open*. 2024;7(7):e2418639. doi:10.1001/jamanetworkopen.2024.18639
39. Tian W, Liu Y, Cao C, et al. Chronic stress: impacts on tumor microenvironment and implications for anti-cancer treatments. *Front Cell Develop Biol*. 2021;9:777018. doi:10.3389/fcell.2021.777018
40. Pan J, Zhang L, Wang X, et al. Chronic stress induces pulmonary epithelial cells to produce acetylcholine that remodels lung pre-metastatic niche of breast cancer by enhancing NETosis. *J Experim Clin Cancer Res*. 2023;42(1):255. doi:10.1186/s13046-023-02836-5
41. Estévez-Cabrera MM, Sánchez-Muñoz F, Pérez-Sánchez G, et al. Therapeutic treatment with fluoxetine using the chronic unpredictable stress model induces changes in neurotransmitters and circulating miRNAs in extracellular vesicles. *Heliyon*. 2023;9(2):e13442. doi:10.1016/j.heliyon.2023.e13442
42. Pondeljak N, Lugović-Mihić L. Stress-induced interaction of skin immune cells, hormones, and neurotransmitters. *Clin. Ther*. 2020;42(5):757–770. doi:10.1016/j.clinthera.2020.03.008
43. Zhang H, Wang Z, Wang G, et al. Understanding the connection between gut homeostasis and psychological stress. *J Nutr*. 2023;153(4):924–939. doi:10.1016/j.tjnut.2023.01.026
44. Han J, Jiang Q, Ma R, et al. Norepinephrine-CREB1-miR-373 axis promotes progression of colon cancer. *Mol oncol*. 2020;14(5):1059–1073. doi:10.1002/1878-0261.12657
45. Zhou Z, Shu Y, Bao H, et al. Stress-induced epinephrine promotes epithelial-to-mesenchymal transition and stemness of CRC through the CEBPB/TRIM2/P53 axis. *J Transl Med*. 2022;20(1):262. doi:10.1186/s12967-022-03467-8
46. Benfield P, Heel RC, Lewis SP. Fluoxetine. A review of its pharmacodynamic and pharmacokinetic properties, and therapeutic efficacy in depressive illness. *Drugs*. 1986;32(6):481–508. doi:10.2165/00003495-198632060-00002
47. Hu J, Teng J, Wang W, et al. Clinical efficacy and safety of traditional Chinese medicine Xiao Yao San in insomnia combined with anxiety. *Medicine*. 2021;100(43):e27608. doi:10.1097/MD.0000000000027608
48. Liu Y, Ding XF, Wang XX, et al. RETRACTED ARTICLE: xiaoyaosan exerts antidepressant-like effects by regulating the functions of astrocytes and EAATs in the prefrontal cortex of mice. *BMC Complement Alternat Med*. 2019;19(1):215. doi:10.1186/s12906-019-2613-6
49. Wang M, Huang W, Gao T, Zhao X, Lv Z. Effects of Xiao Yao San on interferon-α-induced depression in mice. *Brain Res Bull*. 2018;139:197–202. doi:10.1016/j.brainresbull.2017.12.001
50. Li M, Zhang W, Yang L, et al. The mechanism of Xiaoyao San in the treatment of ovarian cancer by network pharmacology and the effect of stigmasterol on the PI3K/Akt pathway. *Dis Markers*. 2021;2021:4304507. doi:10.1155/2021/4304507
51. Zhao L, Zhu X, Ni Y, You J, Li A. Xiaoyaosan, a traditional Chinese medicine, inhibits the chronic restraint stress-induced liver metastasis of colon cancer in vivo. *Pharmaceutical biology. Pharmaceu Biol*. 2020;58(1):1085–1091. doi:10.1080/13880209.2020.1839513
52. Zhou H, Wang K, Xu Z, Liu D, Wang Y, Guo M. Chronic unpredictable stress induces depression/anxiety-related behaviors and alterations of hippocampal monoamine receptor mRNA expression in female mice at different ages. *Heliyon*. 2023;9(7):e18369. doi:10.1016/j.heliyon.2023.e18369
53. Cao W, Wang X, Li H, et al. Studies on metabolism of total glucosides of paeony from Paeoniae Radix Alba in rats by UPLC-Q-TOF-MS/MS. *Biomed Chromatography*. 2015;29(11):1769–1779. doi:10.1002/bmc.3493
54. Takiyama M, Matsumoto T, Sanechika S, Watanabe J. Pharmacokinetic study of traditional Japanese Kampo medicine shimotsuto used to treat gynecological diseases in rats. *J Nat Med*. 2021;75(2):361–371. doi:10.1007/s11418-020-01474-x